An Investigation of the Effect of Curved Cantilever Geometry on Piezoelectric Power Output

Team PISO

Ian Brady, Mikaila Esuke, Liam Mc Carthy, Catherina Samson, Rithik Sebastian,

Mark Wedzielewski, Sanjali Yadav

under the supervision of Rick Blanton

Thesis submitted in partial fulfillment of the requirements of the Gemstone Honors Program, University of Maryland, 2023

Table of Contents

Abstract

Team PISO recognizes an urgent need for new niches of environmentally sustainable energy, and believes that piezoelectric materials offer a small part of a solution. With this consideration, Team PISO has focused on the process of optimizing the application of strain on a piezoelectric component by altering the dimensions of a cantilever beam. Future research in this avenue could focus on a computational model based off of the experimental data collected herein, or more focused optimization of a selected cantilever profile.

In the long term, PISO's research could be applied to energy harvesters to reclaim power from vibrations and deformations, such as sounds and footsteps, as a novel source of renewable energy for implementation in public, heavily-traveled areas. This paper investigates the relationship between the geometric shape of a piezoelectric cantilever structure and its power output from discrete impulses.

To this end, Team PISO created several curved cantilevers to examine the impact of the geometry of a piezoelectric cantilever on its output. These cantilevers were tested on an apparatus that simulated the movement of a footstep and their power outputs compared. PISO concluded that convex cantilevers were the most effective, with the convex spherical geometry outputting 24% more power than the control rectangular geometry.

Chapter 1: Introduction

1.1: The Need for Clean Energy Production

Humanity can attribute its accelerated cultural and technological progression of recent centuries to the command of electrical power. The fundamental discovery of energy and electricity became the foundation on which modern civilization developed. Due to experimentation with basic circuitry in the eighteenth century, societies have been able to reach heights in communication, transportation, artificial intelligence, and manufacturing through engineering and science. However, all of these agricultural and industrial advancements from hundreds of years ago could not have happened without the utilization of natural or manufactured materials to generate power. Most of the world's current methods of power generation rely on exhaustible energy sources like coal and other fossil fuels, the byproducts of which are known to cause lasting damage to the atmosphere and the global ecosystem [1].

Fossil fuels such as coal are utilized through combustion, which expels massive amounts of carbon dioxide into the atmosphere. The excess of carbon dioxide from these processes has lasting effects on the environment, affecting the populations of countless species and changing meteorological patterns more each year. Arctic amplification, the phenomenon that contributes to the melting of ice reserves at the poles, has led to lasting damages in ecosystems around the globe: rising sea levels, devastating wildfires, tumultuous storms, and a continuously growing global temperature [2] [3]. Densely populated areas in countries like China and India are especially affected by air pollution and smog, posing serious health risks for their own residents [4]. Coal and fossil fuels are also depletable, so as the world population and technological developments continue to grow exponentially, the world's supply plummets. Therefore, the need to search for more sources of renewable energy becomes increasingly urgent with time.

1.2: Issues with Existing Solutions

Due to the noticeable pollutive characteristics of fossil fuels and coal, renewable energy has been in high demand in recent years, making it the fastest growing energy source within the United States. The demand for renewable energy is soaring, while the total coal consumption in the United States is decreasing to 11.3 quadrillion British thermal unit (Btu), its lowest recorded level since 1964, and total renewable energy surpassing that with 11.5 quadrillion Btu, being the highest it has been on record. As the use of coal consumption has dramatically decreased over the past 6 years, renewable energy such as solar, wind, biofuels, and hydro have increased significantly over the past 4 years. The year 2019 marks when the use of renewable energy and consumption of said energy has overshadowed that of non-renewable sources such as coal.

This can all be attributed to renewable energy's efficiency and lack of downstream pollution compared to its predecessors. A large number of sources have been discovered and developed to meet this growing need: solar farms, wind farms, hydroelectric generators, and nuclear power plants are the most promising sources of renewable energy thus far, but they all require large start-up costs, impacted by intermittency and are limited to specific landscapes and/or meteorological conditions in order to work most efficiently. One example of this can be seen with solar energy: it specifically requires large sections of land, a substantial amount of water for cooling and cleaning, and continual maintenance to be comparatively productive [3].

Another example can be seen in wind energy. In order for wind energy to work optimally, wind turbines must be located on farms, rural communities, and coastal areas with little to no barriers to obstruct the flow of air. The energy produced by harnessing the wind is immense, but the energy obtained from wind turbines is far away from the cities that actually need the energy, therefore necessitating even more materials and infrastructure which adds to the cost of construction and maintenance.

Additionally, leading sources of renewable energy such as solar, wind, and hydroelectric power require large amounts of land to operate at scale. The process of clearing this land can have deleterious effects on the surrounding environment, which is usually undeveloped natural land due to the aforementioned land requirement. These drawbacks could be mitigated by implementing renewable energy sources within metropolitan areas, but this comes with its own set of problems: competition with residential and commercial buildings limits the scope of such execution to putting solar panels and turbines on rooftops, which reduces the benefit compared to an analogous power plant and puts the choice of installation at the whim of individual landowners.

However, an energy harvesting system based on piezoelectric materials can be easily implemented into a city setting and structure, and would in fact be more effective in public spaces where noise and vibrations are more prevalent. Additionally, the availability of the energy generated through solar panels and wind turbines does not yet stand up to that of fossil fuels, as the technology is still relatively new and is still being improved upon [12]. While these sources of energy are far less detrimental than comparable fossil fuels, none of them fill the commercial niche of efficient, cost-effective low-power generation requiring small startup costs. Energy production using piezoelectric materials may not have the same raw power output or relatively rapid return on investment as sources such as solar and wind, but it adds a renewable source of energy to highly populated locations where these other sources are not always possible to implement. In short, piezoelectric energy fills a niche which bolsters current renewable energy efforts.

In regards to the startup costs associated with renewable energy sources, the initial cost for a nuclear power plant increased in the years of 2002 and 2008 from 2 billion US dollars and 4 billion per unit to approximately 9 billion per unit within the United States. The cost of a solar farm is approximately 3 million, including development. But, on a per acre scale the cost is approximately 500,000 US dollars with the return on investment varying significantly based on location. A source of clean energy usable in urban areas with a low initial cost would fill a yet unused niche in the energy industry, and encourage the global conversion from fossil fuels to renewable energy.

1.3: The Solution

To investigate energy sources with lower startup cost, the team is looking to expand on an until recently overlooked source of power, which can be collected in highly populated areas and with minimal down payment: footsteps [5]. Public buildings, especially transportation hubs, see a huge amount of pedestrian traffic every day [6]. The action of both putting one's foot down and picking it back up causes the floor to move a measurable amount, deforming and producing heat by way of friction. Harnessing the kinetic energy of the movement might prove to be a viable method of energy production in highly trafficked areas, producing enough energy over time to offset the input cost and environmental impacts of production.

The idea of producing energy from pedestrian traffic only emerged within the last ten to twenty years, but there is a good amount of research on the topic outlining the basic principles of harnessing energy with piezoelectric materials, which convert stress into electricity, and converting kinetic energy to electricity with **dynamos** [6].

A few organizations have made a foray into collecting energy from pedestrian traffic, most notably the British company Pavegen, the US government, and the East Japan Railway Company. However, the technology is underdeveloped compared to the alternatives, and so the piezoelectric tiles currently available on the market exist largely as proof of concept, with minimal profit margins [7].

Team PISO seeks to expand the existing body of knowledge on piezoelectric energy and pedestrian traffic energy harvesting in investigating the structure of a piezoelectric transducer for optimal output. With prior research indicating that piezoelectric cantilevers cut to taper outwards from their base outperform the voltage output of regular rectangular cantilevers, PISO further investigates this phenomenon by manufacturing multiple nonlinearly curved tapers. They then tested the performance of each custom transducer to determine the effect of the curve on the piezoelectric power output under non-sinusoidal low-frequency impulses, such as can be encountered with the heel impact of a footstep.

Chapter 2: Literature Review

2.1: Piezoelectricity

Piezoelectricity is an underutilized resource of clean energy, limited mostly to demonstrations and academic papers as well as lacking widespread use as an environmental offset. Like wind power, it has the ability to convert mechanical energy into usable electricity. However, unlike wind power, piezoelectricity also has the property to convert electrical energy back into mechanical energy. These properties, collectively known as the **piezoelectric effect**, are the focus of this project. We want to look at ways that we can use this unique effect to generate renewable energy [8] [9] [10].

When a piezoelectric material experiences mechanical motion or friction, the stress distorts the material and moves electrical charge, which can then be used to create usable electrical energy [11]. This effect is observed because piezoelectric materials have natural dipole moments due to their crystalline structure. This means that there are areas inside of them with concentrations of either positive or negative charge. When the piezoelectric material becomes distorted, so do the dipoles, and an electric charge is generated. Conversely, when an electric current is run through piezoelectric material, the current forces the charges to create a stronger dipole, which in turn distorts the material and exerts a mechanical force.

Piezoelectric materials can come in a variety of forms. They are divided into four different categories based upon their characteristics: ceramics, single crystals, polymers, and composites [11]. Each category has different benefits and drawbacks.

Piezoelectric ceramics are notable due to their remarkable electrical properties and their stability resulting from the formation of a morphotropic phase boundary, a boundary between distinct crystal phases [12]. The most popular type of piezoelectric material, Lead-Zirconate-Titanate (PZT), falls under the ceramic classification. One downside is that ceramics like PZT produce lead-based byproducts when manufactured [13]. While there are ceramics that are made without lead, they are not nearly as effective.

Single crystals are the crystalline counterparts to ceramics. They are preferable to ceramics in cases where there can only be a small amount of material used. One study showed that by using a certain energy harvesting technique, single crystals could output 20 times the amount that a ceramic could [5]. One of the drawbacks of single crystals, however, is that the cost of manufacturing is higher than that of ceramics [11].

Lastly, piezoelectrics that come in composite polymer forms which have differing properties to standard piezoelectrics. Since composite piezoelectrics are a combination of ceramics or single crystals with polymers, they share a lot of the same characteristics with polymers, namely flexibility [14] [15]. However, unlike polymers, composites (as well as the other forms) exhibit the ferroelectric property. As such, composites produce more output in comparison to polymers.

The strength of the electric field produced when a piezoelectric material is stressed is determined by its **piezoelectric constant**, denoted with a lowercase d. The constant is determined by the material used and the direction of the force with respect to the direction of the material's polarization, also called the **coupling mode**. The constant for any coupling mode can be described with respect to four major modes [16] [17]:

- 3-3, where force is applied parallel to the poling direction, the direction of positive polarization.
- 3-1, where force is applied perpendicular to the poling direction.
- 1-4, where torque is applied parallel to the poling direction.
- 1-5, where torque is applied perpendicular to the poling direction.

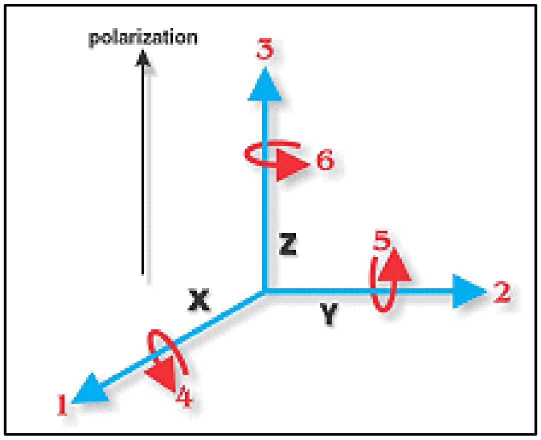

Figure 1. Visualization of coupling modes in the cardinal directions [17]

The piezoelectric constant for each of these coupling modes are denoted d_{31}, d_{33}, d_{14}, and d_{15}, respectively [17]. Each of these coefficients have different values, dictated by the composition of its material. Using these values and vector analysis, the electric field generated from a force of any direction and magnitude can be predicted.

Using the piezoelectric constant, it is possible to calculate the voltage produced by the deformation of a piezoelectric material.

2.2: Impact and Lifespan of Piezoelectric Materials

Piezoelectric ceramics, which have a perovskite structure, are what allows for the conversion of pressure, vibrations, and other configurations of motion into electrical signals. For the purposes of this report, this conversion would allow the conversion of the energy harvested from the force or pressure exerted on the piezoelectric material from human interactions into energy that can be repurposed for other uses [18]. Commonly used piezoelectric materials, which are also piezoelectric ceramics, include PZT, barium titanate (BT), and strontium titanate (ST). Materials that have precedent for the direct application of converting the pressure exerted on piezoelectric floor tiles into energy includes PZT, Polyvinyl Indene Fluoride (PVDF), and quartz.

PZT is unarguably the most effective material for this report's purposes. Compared to its more environmentally friendly counterparts or those who are lead free, it is simply better in terms of raw piezoelectric output. The development of a lead-free piezoelectric material with the equal or better capacities as PZT is expected to take years at best; however, with restrictions to using hazardous materials (like lead) rising in the world, development of these materials is on the forefront of many minds and research. PZT is a (solid) combination of lead zirconate (PZ) and lead titanate (PT) which both have great piezoelectric properties which contribute to PZT's overall peak performance [19] [20].

It is proven that lead can be toxic to people, living organisms, and the overall environment, leading lead poisoning to be a notable environmental health consideration. The main way in which people are exposed or suffer from lead poisoning is from inhaling or ingesting lead. PZT has the potential to be dangerous because of its volatilization at high temperatures; during the production processes of calcination and sintering, PZT can produce trace amounts of lead which cause pollution [21]. In addition, PZT submerged in water has been observed to have left trace amounts of lead in the water supply. It is therefore important for PZT to be well contained during production and usage to minimize negative environmental impact.

PVDF is a polymeric material that can be used in tandem with PZT for power generation and or energy harvesting. As a piezoelectric material, quartz is more precise but has a higher cost compared to PZT and other piezoelectric ceramics. PVDF also has a smaller elastic modulus and therefore is more prone to breakage than PZT. It has a high availability and therefore a precise frequency response, making it more effective when compared to its other piezoelectric material counterparts [22] [23].

Bismuth-based ceramics (BLSF), sodium potassium niobate (KNN), and NBT ($Na_{0.5}Bi_{0.5}TiO_3$). KNN ((K, Na) NbO_3) is a solid combination or solution of NN ($NaNbO_3$) and KN ($KNbO_3$) compounds [24]. KNN is believed to be the more environmentally safe alternative to PZT, but some research indicates that KNN in the early stages of its life cycle can actually be just as or more environmentally harmful than PZT [25] [26].

In terms of usability and lifespan of these piezoelectric materials, PZT is actually not suited for frequent cyclic loading. PZT can be considered a brittle material as an inorganic ceramic and must be protected from either strenuous or harsh environments. If PZT is overexerted, it loses a significant amount of piezoelectric properties but may not have visible deformation or cracking. However, PVDF can be considered virtually unbreakable when exposed to these same strenuous conditions and quite long lasting. PVDF as a polymer material is comparatively flexible, with an elastic modulus 25x smaller than PZT, which makes it more resistant to both mechanical stresses and destruction forces [16] [21] [27].

2.3: General Applications of Piezoelectric Material

The converse effect of piezoelectric materials to exert force when exposed to a voltage is well-documented and often used in a broad range of industries, especially where precision is involved. Atomic force microscopes, ultra-precise machine tools, actuators, and structural damping mechanisms all take advantage of piezoelectric materials for their capacity to make small adjustments to their shape as the electric field around them changes [16]. On the other hand, their direct effect of creating a voltage when deformed is relatively underused until recently, as research has mostly been focused on technologies that promise to yield larger quantities of power.

That said, piezoelectric power generation does exist. The most widely used piezoelectric material in energy harvesting is the aforementioned PZT, which is both easy to manufacture and capable of generating a large amount of energy compared to other piezoelectric materials, due to its large charge coefficient [22].

Piezoelectric power harvesting largely makes use of piezoelectric materials coupled in the 3-1 mode or the 3-3 mode, since these coupling modes generally have the largest charge coefficients out of the four listed in the previous section. Generators in different modes work best under different circumstances [28]. For example: 3-1 generators, often designed as vibrating plates or rectangular cantilevers, have a lower charge coefficient but are easier to make vibrate at resonance. This allows them to be more responsive to low-frequency or low-amplitude vibrations, or irregular inputs. 3-3 generators, often arranged as several alternating layers of **piezoelectric wafers** and electrodes, have a higher charge coefficient but vibrate less freely, making them well-suited in situations with high-powered, regular inputs which drive their oscillation [29] [30].

Any type of piezoelectric generator operates at peak performance when exposed to a vibration of the same frequency as its resonance. At resonance, the piezoelectric material experiences its maximum deformation as it vibrates, and so outputs the maximum amount of voltage it is theoretically able to. As the vibration of the system strays away from resonance, piezoelectric output drops sharply, especially if the system's vibration becomes lower than the resonance frequency [27]. This is a consideration for piezoelectric floor tiles, since pedestrian traffic typically occurs at low frequencies and irregular intervals.

2.4: Piezoelectricity in Floor Tiles

The properties of the piezoelectric effect have the potential for use in many fields, but the focus of this project is utilizing piezoelectric materials to generate energy through a floor tile. The general concept of this consists of creating an area of floor which contains piezoelectric materials which will interact with pedestrian traffic, thus generating current. While this idea has seen minimal application so far - restricted only to isolated uses in very specific facilities - various researchers have conceptually designed or prototyped floor tiles which implement piezoelectric energy generation.

Piezoelectric floor tiles typically are multilayered constructs: the actual piezoelectric material is placed on the surface where it can receive mechanical input, and circuits are placed below this layer for spacing, usually in the form of a converter where the produced current is made usable in some way [31]. The surface layer is allowed to deform, while the circuit layers underneath are made rigid and stable.

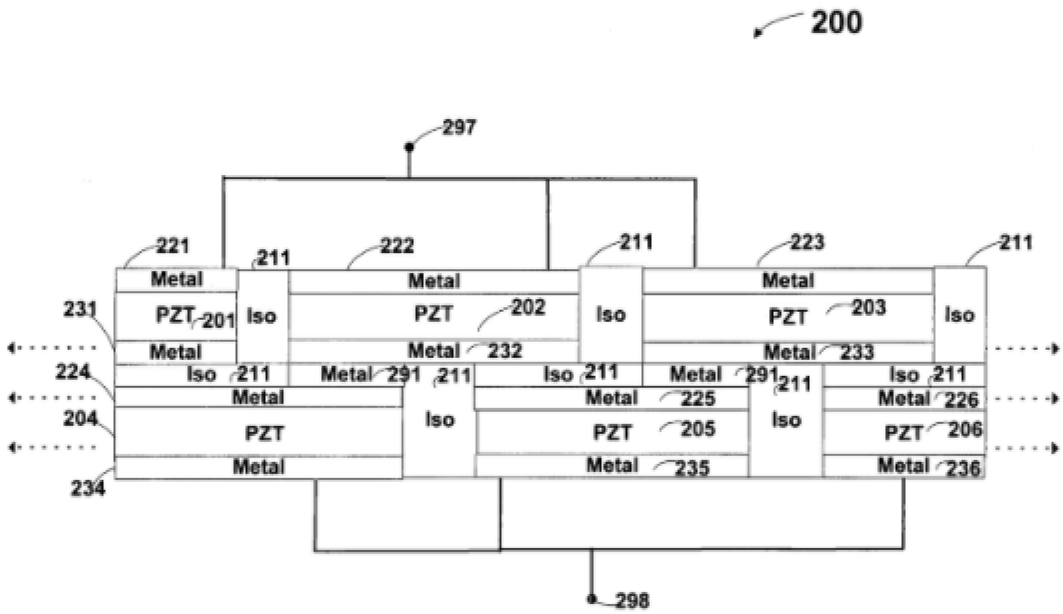

Figure 2. Example of Piezoelectric Tile layering [32]

Actual piezoelectric floor tiles have mostly been made for demonstrative purposes due to the relatively slow rate of energy generation, but efforts have been made to integrate these tiles with other generation methods for more optimal output. It has been attempted to add **photovoltaic cells** to the top layer, thus allowing the surface layer to act as both a piezoelectric generator and a solar generator [33]. This potentially supplements outside floor areas by allowing the tiles to generate energy, even when pedestrian traffic is relatively low; this concept could receive use in outdoor train stations or market areas.

Other prototypes have explored implementing magnetic inductors, which would be affected by the moving charge from piezoelectric displacement to create additional induced current [34]. Since **magnetic induction** would use some already existing functions of a piezoelectric tile to produce current - instead of adding completely new circuits - the efficiency of the piezoelectric tile with regard to its basic form is increased.

Furthermore, while efficient piezoelectric tiles presents a good first step, research groups such as one at Tongji University in China, as well as the Israel-based Innowattech, have looked into applications of piezoelectric traversal energy general for other surfaces, such as roads and railways [35]. While these surfaces may not see high pedestrian traffic like walkways, they are frequently traveled over by heavy vehicles, which can easily provide piezoelectric charge with regularity. Any efficiency boost to piezoelectric generator systems has the ability to increase the technology’s applicability, and thus its impact on alternative power production.

2.5: Optimizing Piezoelectric Floor Tiles

The energy generated from piezoelectric tiles depends significantly on foot pressure distribution while walking, duration of pedestrian traffic, shape of the tile, energy harvester model, and shape of the cantilever. In order to optimize the output of the tiles, these factors need to be taken into account.

Analyzing pedestrian traffic is an integral part of maximizing the input for piezoelectric tiles. There is a vast difference in the foot pressure distribution during walking between young and old adults. The elderly (60+ age) have lower maximum pressure and force as compared to the young (20 - 40 age) population [36] [37]. Since pressure is a key element in maximizing energy input, it is important to consider factors that can increase or decrease the pressure.

Additionally, input energy can be increased if the tiles receive consistent pedestrian traffic. In fact, consistent traffic for a shorter duration (4 hours) generates twice as much energy as compared to an inconsistent pedestrian traffic for a longer duration (12 hours). Every time the piezoelectric tile senses a footstep, the downward force drives an energy-storing flywheel inside the tile, which spins to convert kinetic energy into electrical energy [38]. It’s like a generator in motion and with consistent load, the energy generated will be much higher as compared to inconsistent pedestrian traffic. Thus, installing piezoelectric tiles on crowded walkways or dance floors will generate more energy as the traffic pattern is more consistent. Further, lobbies and common areas in apartments and offices are also good candidates for receiving consistent pedestrian traffic for certain intervals of the day [39].

The shape of the piezoelectric tile significantly affects the energy output. Pavegen, an established company, is using kinetic technology for generating energy from footsteps [40]. They changed their tile shape from square to triangular because they are able to capture much more energy with triangular tiles [25]. Each footstep triggers three or four generators in the Pavegen floor tiles [38]. With their square tiles, only 20% of steps would fall in the right place and trigger the generators. However, with triangular tiles, they are able to achieve 100% accuracy. Thus, the shape of the tile is a crucial factor in optimizing the piezoelectric tiles.

The piezoelectric harvester can be coupled with other types of harvester to amplify the energy output. For instance, a piezoelectric-thermoelectric hybrid energy harvester can collect energy from two different types of sources: thermal and kinetic. By harvesting from two different sources at the same time, the total harvested energy is increased. Even when one of the energy sources is not present, harvesting energy from another source continues and it allows for an uninterrupted energy collection [7]. Therefore, a hybrid energy harvester is more beneficial.

Another major factor in the output of a piezoelectric floor tile is the shape of the cantilever used within the tile. Ideally, the proper cantilever shape should be able to maximize output while similarly minimizing costs. While altering the shape of the cantilever might not maximize the power output of a piezoelectric floor tile, it may decrease the price per area of the piezoelectrics used within the tile. This would conceivably make the piezoelectric floor more accessible to lower income communities. It has been empirically shown that altering the shape of the piezoelectric cantilever beyond a rectangular profile changes the peak power output of the cantilever, to the effect that certain shape alterations use <60% of the mass, but have a >40% power increase [41]. Moreover, these alterations also tend to lower the resonance frequency of the cantilever. This gives promising results as lower resonance frequency, higher power output, and fewer used resources are all beneficial for the prospect of using piezoelectrics in floor tiles.

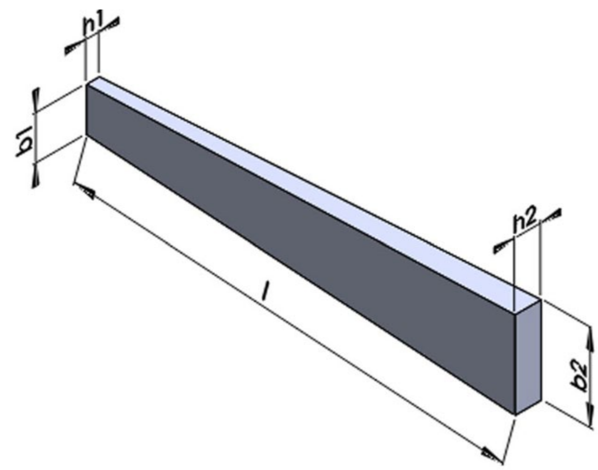

Figure 3: An example of a linearly tapered piezoelectric. This particular configuration demonstrates a 45.14% increase in voltage over a rectangular cantilever of cross-sectional area h2 x b2. [41]

In conclusion, pedestrian traffic, foot pressure, tile shape, energy harvester model, and cantilever shape are key players in optimizing the output of piezoelectric floor tile. Of these, we observe the most potential in optimization of energy output by altering the shape of the piezoelectric cantilever.

2.6: Power Generation and Storage

Electrical energy storage is the process of converting energy from one form (usually electrical) into a storable form that can be held in a medium and converted back to electricity to use [42]. There are a variety of options for storing energy: including compressed air, pumped hydro, or supercapacitors. However, this project will most likely involve the use of batteries, known to be excellent for integration in renewable energy collection [43]. Their energy transfer does not generate carbon emissions, they are flexible in power and energy characteristics, have long cycle lives, and are low maintenance, all of which align with the ideals of this project.

Batteries have a primary use as support for large scale renewable energy storage, such as solar or wind, because they stabilize and regulate frequency in order to interface the system's output with the rest of the grid [44]. One study also found batteries had the lowest power interface costs among energy storage systems [45], which means that it is cheapest for batteries (specifically Nickel-Cadmium batteries) to convert the electricity they generate into storable energy.

This leads to an important point, there are a wide variety of battery types available to use in this study. One type of battery we investigated was the flow battery. Vanadium redox flow batteries are considered useful for small-scale battery energy storage systems [44] and have lower levelized costs of delivery (which involves a ratio between the storage system's cost and its electrical output over its lifetime) [46]. Alternatively, Lead-Acid batteries score consistently for bulk energy storage, distributive storage, and power availability [47].

However, while batteries do not produce carbon dioxide directly through their use, they can have a variety of negative environmental impacts, which in part depend on the type of battery used. For instance, while Nickel-Cadmium batteries are highly effective at storing electrical energy, the cadmium they contain is highly toxic and notably damaging to aquatic environments. They have been replaced with Lithium-Ion batteries in most places, noted for their "high energy efficiency, high power density, and environmental friendliness" [48].

Specifically LFP (LiFePO4) batteries are widely praised for their low cost, high safety, and long cycle lives. These traits align strongly with the project's goals of creating a relatively inexpensive and long lasting form of energy generation and storage. The carbon footprint of Li-Ion batteries is further reduced because they can be recycled [49]. The Lithium-Ion battery recycling industry has been expanding, as the need grows with the increase in electric vehicles in use. As such, when the life cycle of a tile does finally complete, the user should be able to return the battery to a designated location to minimize the environmental impact.

2.7: Piezoelectric Equations

This project will use various piezoelectric equations to make important calculations for the creation of tiles. Here are some equations encountered in the research that have been deemed potentially valuable as the team constructs its own models and performs experiments.

The equation for strain in a piezoelectric material is as follows:

$$S_p = s_{pq}^E T_q + d_{kp} E_k$$

In this equation, S is the strain, T is the stress (pascals), E is the electric field (volts/meter), s is the elastic compliance in a constant electric field (1/pascal), and d is the piezoelectric constant (meter/volt).

The equation for electric displacement in a piezoelectric material is as follows:

$$D_i = d_{iq}T_q + \varepsilon_{ik}^{T}E_k$$

In this equation, E is the electric field (volts/meter), T is the stress (pascals), D is the electric displacement (Coulombs/meter^2), d is the piezoelectric constant (meter/volt), and ε is the permittivity of the material at constant stress (Farad/meter).

The equation for charge in a piezoelectric material is as follows:

$$Q = -\int \int D_3 dA = -\frac{1}{t_p}\int \int \int D_3 d\Psi$$

$$= -\frac{d_{31}}{t_p}\int \int \int T_1 d\Psi + \frac{\varepsilon^{T}{}_{33}A}{t_p}\cdot V$$

$$Q = -\frac{d_{31}}{t_p}\int \int \int T_1 d\Psi + C_p V$$

Where Ψ is volume, $V = -\int E_3 \times dz$, and defined $C_p = \frac{\varepsilon^{T}{}_{33}A}{t_p}$.

In this equation, Q is the charge (coulombs), t is time (seconds), T is the stress (pascals), D is the electric displacement (Coulombs/meter^2), d is the piezoelectric constant (meter/volt), and ε is the permittivity of the material at constant stress (Farad/meter). All other components are explained in the image.

Magnetic induction may be used in components to increase efficiency. The equation for magnetic induction in a piezoelectric material is as follows:

$$B = d^{*}{}_{33}\sigma + \mu^{\sigma}H$$

In this equation, B is the magnetic induction (tesla), Sigma is the compress stress (pascals), Mu is the relative magnetic permeability at a constant stress (Henry/meter), H is the magnetic field (tesla), and d33 is the parameter of the magneto-mechanical effect:

$$d^{*}_{33} = \partial D/\partial\sigma|_{H=const}$$

2.8: Summary

Our project will be developing the underutilized clean energy source of piezoelectricity. The piezoelectric effect allows for the conversion between mechanical and electrical energy, and is exhibited in a variety of materials. Each classification of material has its own properties, with unique benefits and drawbacks.

The use of piezoelectric materials to generate electricity is currently very limited. Therefore, this study is meant to expand on the knowledge of piezoelectric tiles for energy harvesting. It will primarily focus on optimizing the performance of existing piezoelectric technology.

There are other ways to increase the efficiency of the piezoelectric device. For example, the floor tiles should be strategically placed to maximize energy collection, as well as specifically designed to harvest as much energy per footstep as possible. Lastly, the energy harvesting mechanism can be improved to minimize the wasted energy in the conversion process.

Lastly, energy storage is an important component of piezoelectric tiles. Batteries provide an attractive option, due to their variety of properties as well as their history of being integrated into large-scale power generators. However, the method used should be chosen conscious of environmental concerns and ease of access to the design, through low maintenance and simple installation.

Chapter 3: Methodology

3.1: Research Questions

In order to effectively conduct the optimization testing required to realize Team PISO's ultimate goal of making foot traffic a viable energy source, the team has developed three research questions to guide our studies and focus our efforts:

1. How can existing piezoelectric energy harvesting technology be improved?
2. How can we optimize the shape and design used in order to maximize energy production?
3. Does the geometry of the tapered piezoelectric transducer affect the energy output?

These questions have been used as a baseline gauge of progress and as a guideline for planning future steps in the project and where to focus for maximum effect.

While not necessarily a guiding question for research, this question was important to keep in mind as the project continued, in order to avoid straying from the end goal or focusing too much on one avenue of testing and creating a substandard final result with minimal applications in the real world. Every step of the way, the team considered how the gathered data differs in the context of the real world, as opposed to our simulation.

Within the study, the overarching question or thought has been whether it is possible for us to improve on the technology for piezoelectric floor tiles in order to make them viable sources of energy. In order to both analyze and answer this question, the team has conducted multiple experiments to collect data to determine the effectiveness of the technology.

3.2: Design Iterations

3.2.1: Experiment Intent

In order to derive solutions to our research question of ‘how can piezoelectric energy harvesting be improved?’, the team realized that they would need to produce a mathematical model that characterizes the behavior of a piezoelectric tile: in terms of both the mechanical forces experienced by the tile and resulting electrical output. In order to validate this model, the team required a simple and consistent mechanical input. To accomplish this, a series of testing apparatus were constructed that were designed to elicit repeated outputs from the piezoelectric tile. The two most significant iterations of the design are described below.

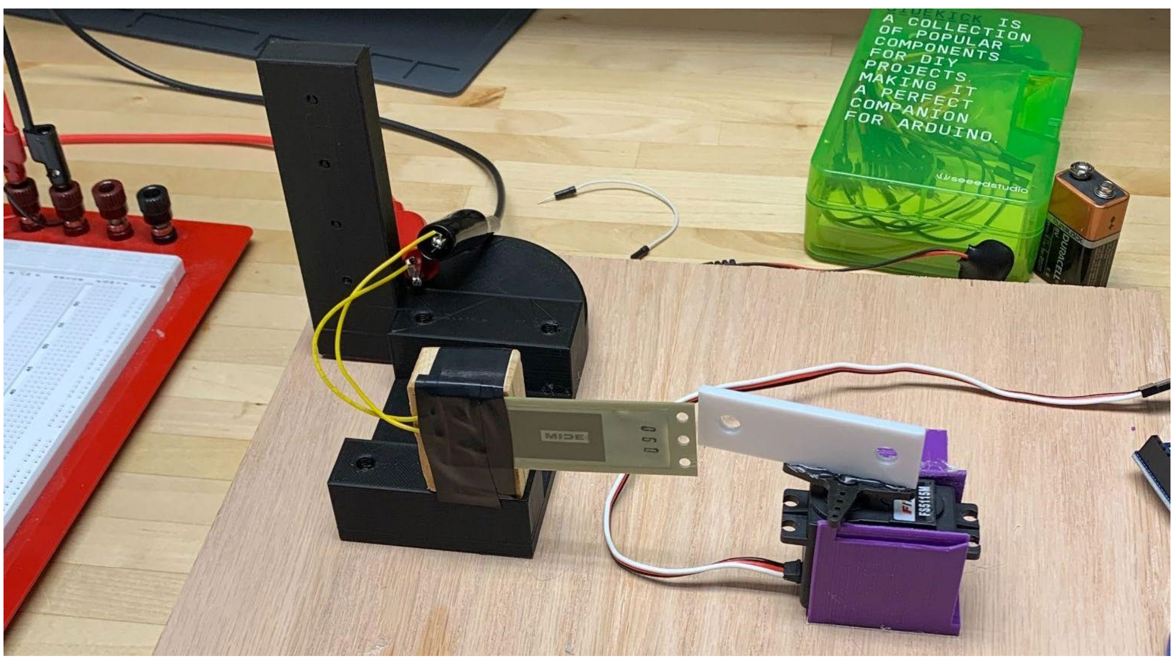

Figure 3. Initial Apparatus Prototype Construction

The initial design for the apparatus consisted of a bar of solid material with its end mounted to the output shaft of a stepper motor (Figure 3). The piezoelectric tile then had its end mounted to another block of material, which was attached to the base. The motor was mounted, in a specially designed plastic motor holder, to the final mass of material which in turn was attached to the board. These two blocks were spaced apart so that only short sections of the ‘arm’ attached to the motor and the cantilevered piezoelectric could contact each other.

The motor was then plugged into a circuit using an L293D motor driver and powered by an Arduino (Figure 3). The code uploaded to the Arduino allowed the user to change the speed of the motor by changing a variable before uploading from the computer. The piezoelectric was then wired into a KeySight InfiniiVision DSOX2024A oscilloscope, which produced a graphic showing the voltage generated within the piezoelectric over the course of the experiment. The data was also saved to a portable drive as a .csv file, which could then be analyzed.

This testing apparatus was capable of producing a consistent output from the piezoelectric. It accomplished this by imparting consistent forces on the tile by swinging its arm into the piezoelectric to induce a bending motion. It was capable of doing this by swinging the arm back and forth through driving and reversing the direction of the stepper motor.

This model also had a number of weaknesses. It was primarily hampered by the materials used in its construction. Wood was used for all the solid masses: the two blocks that held the piezoelectric tile and the motor in place and the base of the apparatus. The swinging arm was built from a leftover 3D printed part. Additionally, the piezoelectric tile was mounted to the wooden block using tightly drawn tape. While this was effective in holding the piece in place for some time, after enough trials the tape would begin to fray or come undone, and the tile would shift slightly. The final, and most important, issue with this design was that it allowed the piezo to oscillate back and forth after it was depressed. Once the arm moved off of the tile, the piezoelectric would spring back and then vibrate. This would cause bending in the opposite direction, which induced voltage with a negative sign and was not indicative of how the piezo would behave if it were actually installed in a floor tile.

Figure 4. Tinkercad of Second Apparatus

3.2.2: Second Apparatus Construction

The most recent iteration of the testing apparatus demonstrates a clear evolution from the initial prototype. In this design, instead of striking the piezoelectric tile, the group elected to use a rolling mass to displace a section of the piezoelectric and induce bending. The roller was a specially designed 3D-printed part that consisted of a shaft with a cylinder attached, off center. This way, as the shaft is rotated the cylinder will stick out more or less depending on its angular position. This shaft is supported by a 3D-printed plastic frame and driven by a chain connecting

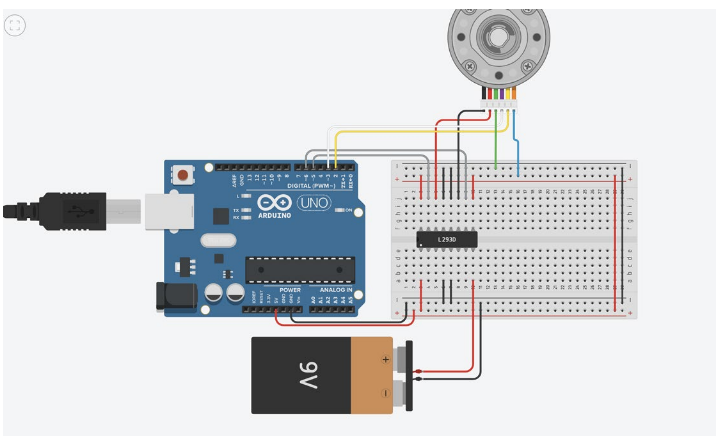

to a Pololu 37Dx65L 24V Gearmotor. This motor is controlled by an Arduino, but the circuit connected to it has now integrated a potentiometer and button that allow the user to shift or set the motor speed during operation.

The piezoelectric is screwed down to the plastic frame and still in a cantilever position. The same oscilloscope is used, as well as the same data analysis method. A micrometer was incorporated into this design to give precise control over the deflection caused by the rolling component. The rolling component could then occupy overlapping space with a slot for mounting a piezoelectric component during part of its rotation cycle. This configuration has resulted in piezoelectric outputs much closer to what is expected by the team.

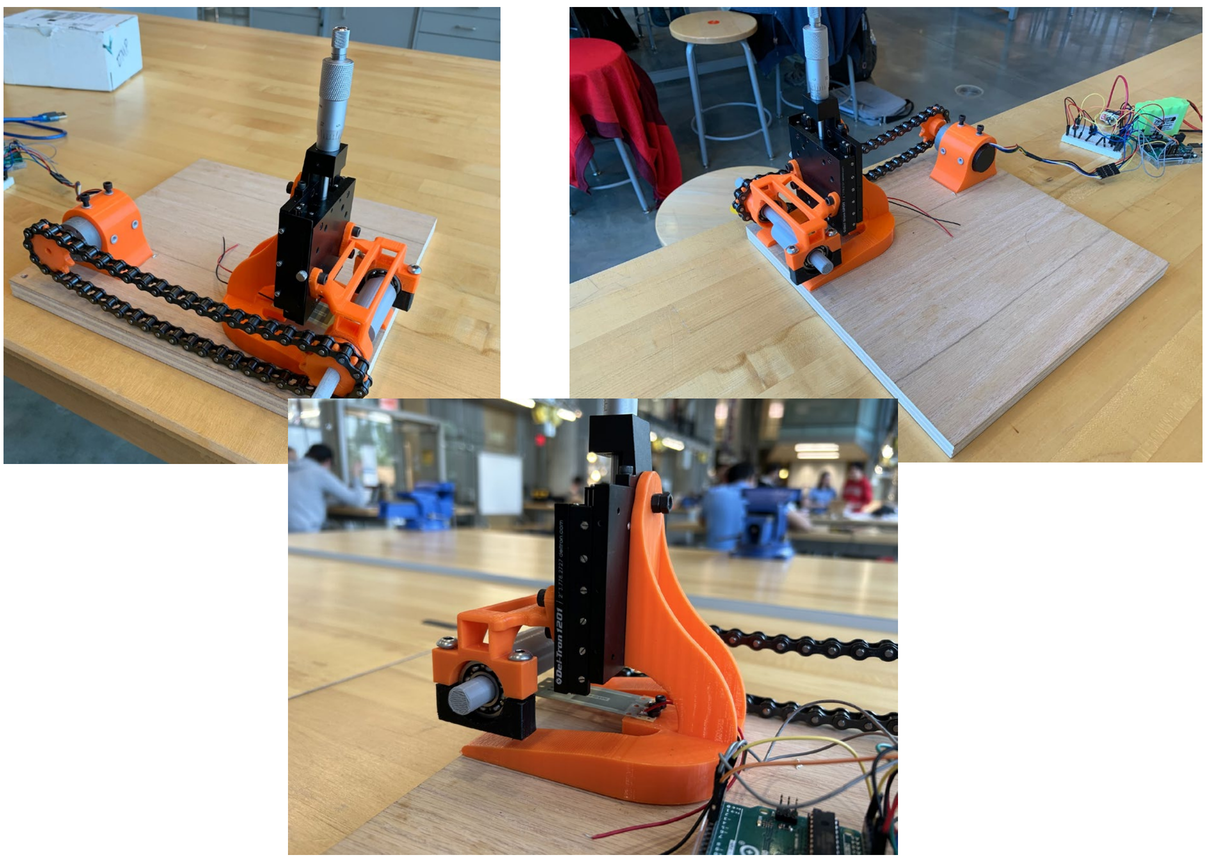

Figure 5a. Second Testing Apparatus

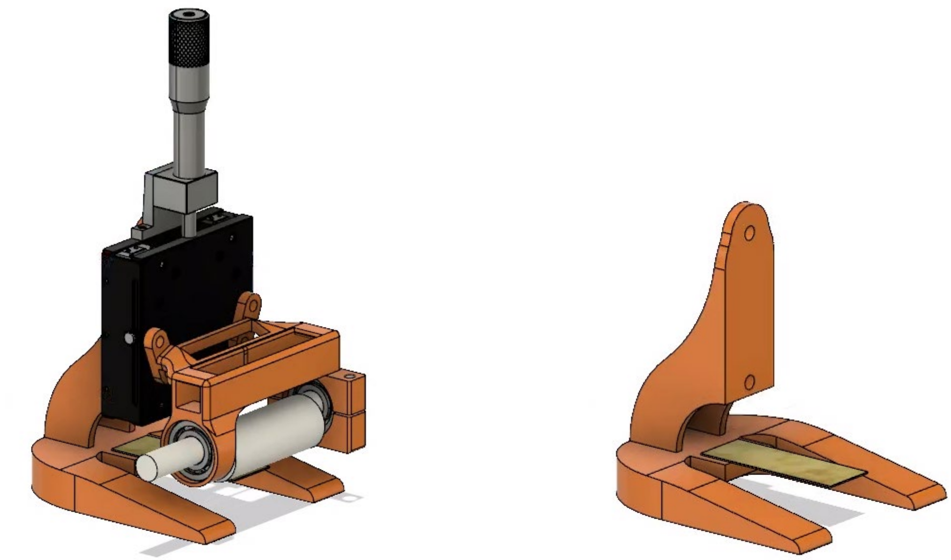

Figure 5b. Second Testing Apparatus (CAD Model) showing the placement of the piezoelectric wafer within the testing rig

3.3: Lab Experimentation and Physical Testing

Due to the fact that our project is centered around engineering and development, the proposed research design for this project would consist primarily of lab research and conducting experiments on varying geometric designs in order to optimize the voltage output.

In order to collect data on the piezoelectric constants and energy outputs of the materials, a motor-driven press was used to apply a specific amount of force to a piezoelectric component in order to gauge its effectiveness. The research team produced a testing procedure to standardize the process of taking data readings from a number of different piezoelectric wafers with different geometric designs. As described previously, this apparatus used a mounted micrometer to force an off-center cylinder to push the cantilever down a selected amount. The cylinder was driven by a motor which had a rotation speed set and real-time corrected by an Arduino board.

The procedure for acquiring data for each wafer is included. Each piezoelectric wafer has two leads installed, in order to integrate it into a circuit to take the voltage difference reading. The wafer was fastened to the board using screws. For each test, the micrometer was set to a particular height and recorded, controlling the displacement experienced by the cantilever. The program used to control the test apparatus utilized pulse width modulation (PWM) in order to attain particular rotational frequencies for the motor. These frequencies were set and recorded. The leads from the wafer were then installed into a breadboard in series with a 220 kΩ resistor.

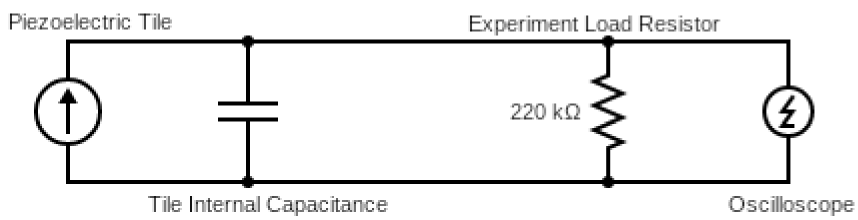

Figure 6. Experiment Circuit Diagram

The probes from the oscilloscope were attached across the resistor to measure the voltage difference. This value was recorded for the duration of the test: 1 second for each individual trial. These trials were modified to record how the voltage difference changed depending on the maximum possible deflection and the motor speed. The micrometer and PWM values were changed and recorded between trials in order to produce the full data set.

3.4: Data Collection Through Simulations

In order to fully answer our research questions, we needed to consider additional data to gauge our own. To use as a basic guide on the accuracy and correct shaping of our results, we created a simulation to approximate the output of the second apparatus.

Using the following equation, we calculated the maximum deflection for a given applied force: $\delta_{max} = \frac{FL^3}{3EI}$. In this equation, δ_{max} is the maximum deflection, F is the applied force, L is the length of the cantilever, E is the Young's Modulus of the cantilever, and I is the moment of inertia for the cantilever. By simulating applied forces over times, we produced graphs of deflection vs time, such as the following:

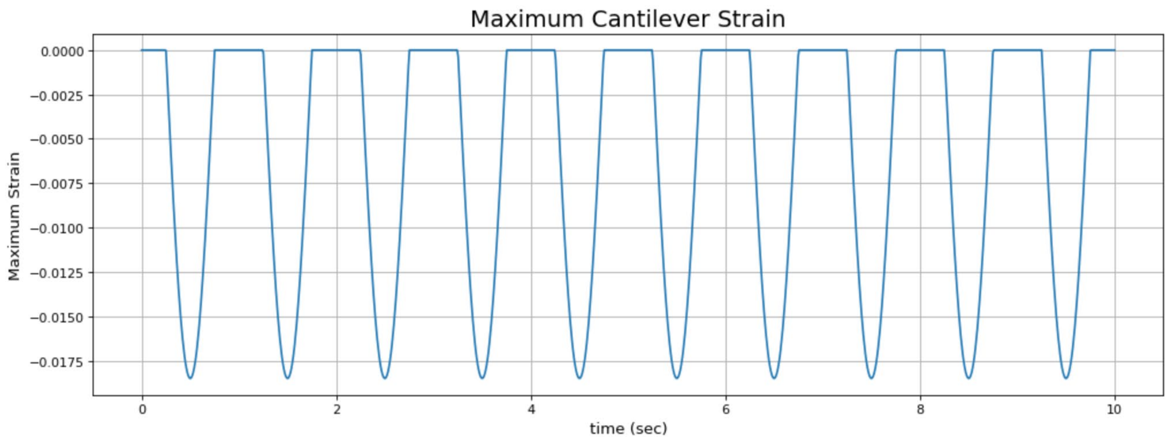

Figure 7. Deflection vs. Time Graph from Simulations

By applying this to calculate strain, we simulated a graph of the same shape but different scale. This was applied to find voltage using the equation: $V = \frac{n_p t_c d_{31} Y}{\varepsilon} \varepsilon'$ [50]. In this equation, V is the voltage, n_p is the transformer constant, t_c is the piezoelectric material thickness, d_{31} is the piezoelectric charge constant, Y is the admittance of the circuit, ε is the strain, and ε' is its first derivative with respect to time.

This produced the following graph of voltage vs time:

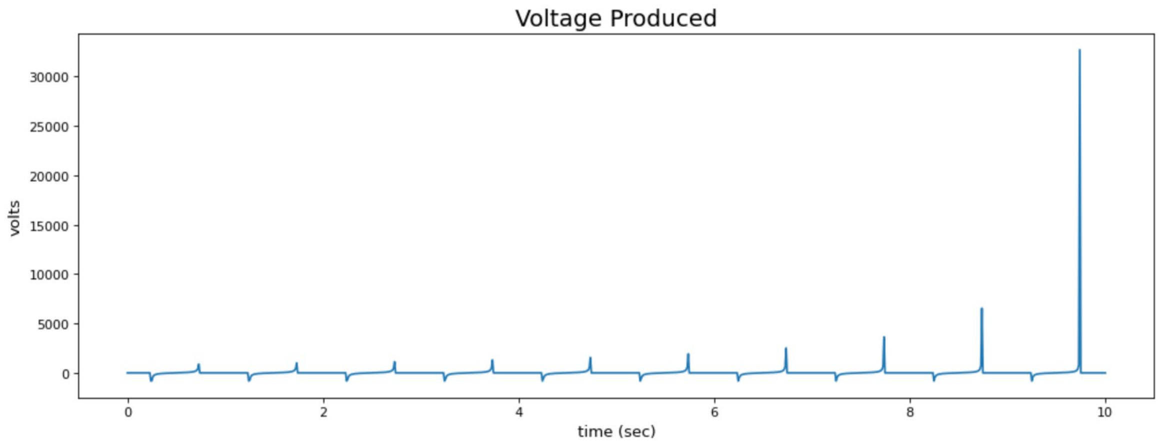

Figure 8. Voltage vs. Time Graph

This graph was not accurate to our results, but did serve as a way for us to investigate the properties of piezoelectric materials and refine our literature review. Unfortunately, we did not manage to produce a viable simulation which matched our results and this was not used in our final results.

3.5: Specialized Subteams for Optimum Research

Our chosen design involved using the rotating cylinder test apparatus on differently shaped piezoelectric material to determine how the shape of the material had an effect on the output power of the system. The intent was to determine if a piezoelectric cantilever of a particular shape could be implemented in a tile for greater electrical returns via the conversion from external mechanical motion. While our literature search returned studies which did such based on the mass distribution of the cantilever, these all used consistently sized piezoelectric materials which did not change shape to match the cantilever. To expand on this area, we used different piezoelectric components which tapered according to distinct mathematical curves.

To contribute to this goal we distributed our efforts into three sub-categories, which were focused on, to different degrees by separate members of our team, forming subteams. The first of these three subteams focused on construction, as data collection would be limited without apparatus materials that needed to be created. This included components of the rotating cylinder design used to test cantilevers, as well as the cantilevers themselves. Main apparatus components were designed in CAD software and 3D-printed, while shaped cantilevers were cut from existing piezoelectric cantilevers using a computer-guided water-jet cutting tool.

The creation of these materials allowed the second team to perform data collection on the cantilevers, running tests on the cut piezoelectrics to obtain empirical data. This formed the basis of our findings.

The third of these three subteams focused on modeling, using equations in the literature to create a computer-simulated approximation of the output of the piezoelectric tile in our desired circumstances. Through this, we could obtain a better idea of the general desired data to expect from physical data collection. Additionally, feedback from the data collection team could be used to compare whether a certain parameter change resulted in positive or negative progress. We could then adjust our approach accordingly by bringing said feedback around the construction and data teams to re-evaluate which designs made the most sense.

3.6: Cantilever Curvature Profiles

To investigate the effect of a curved taper on the performance per area of a piezoelectric cantilever element, three simple mathematical curves were elected as test candidates: spherical, exponential, and sinusoidal. These different geometry types would lead to similarly curved but uniquely varied cantilevers which would serve to examine how these fine adjustments of shape resulted in potentially different outputs. To create specimens of each curve, rectangular piezoelectric cantilevers were cut using a waterjet into tapered curves of each geometric type, expanding from a 0.5-inch width to a one-inch width over a length of 2.25 inches. Curves were only cut in the length and width dimensions, whereas the thickness of the cantilevers were kept at their initial dimension of 0.71mm thick, of which only 0.15mm of the thickness was piezoelectric material. Each curve specimen was cut in two variations – concave and convex – in order to identify any differing performances based on mass distribution or mechanical stress. Additionally, a cantilever was also cut with a linear taper. Finally, an unmodified rectangular piezoelectric wafer was tested as a baseline to establish a control for the experiment. Figure 9 displays the wafers after each of the described cuts.

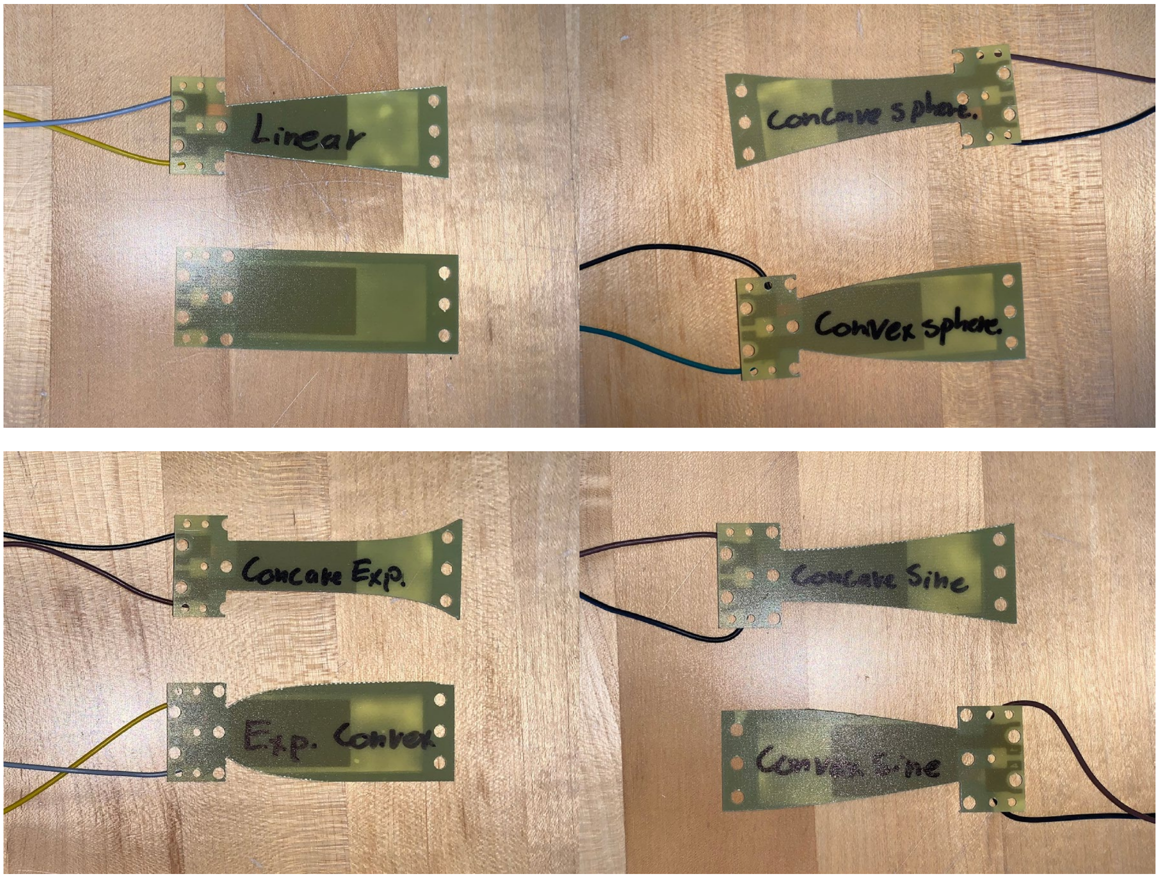

Figure 9: The eight cuts used in experimentation: linear cut and rectangular uncut (top left), concave and convex spherical cuts (top right), concave and convex exponential cuts (bottom left), concave and convex sinusoidal cuts (bottom right).

The curves used were generated manually, by using the known dimensions of the rectangular cantilevers to describe mathematical formulae which intersect with desired points on the cantilever surface. Once the curves were established mathematically they were transcribed into SolidWorks as equation driven curves, then converted into DXF files, a format legible to the waterjet cutter.

To offset the differences in voltage output brought about by the different curve specimens containing different masses of piezoelectric, the surface area of each specimen was measured for use in determining a specimen's maximum voltage per surface area. In this way, each curvature variation can be graded by both its total voltage output and its potential density.

Each specimen was tested at variable impulse frequencies, ranging from 3 to 7 Hz in one-Hz intervals, at a maximum vertical displacement of 2.333 mm. These frequencies were not chosen for any purposes of resonance frequency analysis, but because they approximate the rate at which a piezoelectric tile would be stepped on. Additionally, each specimen was tested at variable vertical displacements, ranging from 0.333 to 4.333 mm in 1 mm intervals; at a baseline frequency of 5 Hz. For each permutation of frequency and displacement, a Butterworth low-pass filter was applied to multiple sets of data to reduce noise and isolate the voltage of each impulse.

3.7: Internal Resistance

Pursuant to the second research question (How can we optimize the shape and design used in order to maximize energy production?), a short test was also conducted with the intent of measuring the piezoelectric's internal resistance in order to approximately calculate the number of piezoelectric units wired in parallel to achieve an acceptable charge rate for conventional power storage options. To this end, the voltage of a rectangular cantilever was tested at 6Hz and 2mm displacement, loaded with successively larger resistances. The open circuit voltage was also taken under the same conditions, to the end of using Thevenin's theorem to calculate an unmodified cantilever's internal resistance.

Chapter 4: Results

4.1: Cantilever Measurements

The area measurements of each piezoelectric geometry are described in Figure 10. The Area value describes the total area of each piezoelectric wafer, including the space for the fasteners. The Piezoelectric Area describes the area of the piezoelectric shim within the wafer. The Standard shape has not been modified from delivery. The relationship between the two is direct. The largest cut wafer was the Exponential Convex. The smallest cut wafer was the Spherical Concave.

The inherent inaccuracy of the waterjet used to manufacture the piezoelectric components (A ProtoMAX abrasive waterjet) is the dominant contributor of error in this measurement. With a linear inaccuracy of ±0.127mm, the uncertainty of a cantilever area carved out by this instrument can be approximated by applying the linear inaccuracy as the uncertainty of the cantilever's rectangular dimensions:

$$\sigma_A = (lw) * \sqrt{(\frac{\sigma_l}{l})^2 + (\frac{\sigma_w}{w})^2}$$

$$\sigma_A = (25.4 * 71.0) * \sqrt{(\frac{0.127}{25.4})^2 + (\frac{0.127}{71.0})^2} = 9.6 \text{ mm}^2$$

Similarly, for the piezoelectric area:

$$\sigma_A = (20.8 * 46.0) * \sqrt{(\frac{0.127}{20.8})^2 + (\frac{0.127}{46.0})^2} = 6.4 \text{ mm}^2$$

Other measurements, such as the 0.03mm^2 measurement error of SolidWorks' area estimation, are several orders of magnitude smaller than that of the waterjet, and thus can be safely ignored.

Geometry	Area [mm²]	Piezoelectric Area [mm²]
Standard	1805±0.3	956±0.3
Straight Edge	1444±9.6	837±6.4
Exponential Concave	1198±9.6	635±6.4
Exponential Convex	1690±9.6	946±6.4
Sinusoid Concave	1345±9.6	757±6.4
Sinusoid Convex	1534±9.6	886±6.4
Spherical Concave	1321±9.6	739±6.4
Spherical Convex	1563±9.6	899±6.4

Figure 10. Sectional Area of all piezoelectric component geometries

The difference between the two areas is illustrated in Figure 11. These values were used to normalize the power output per unit area.

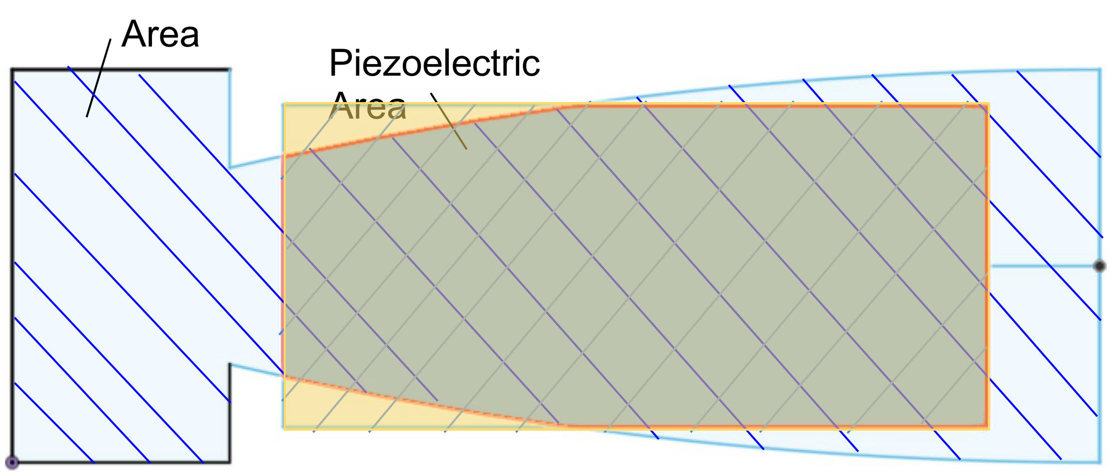

Figure 11. Comparison of Piezoelectric Area

4.2: Power Outputs

Each combination of shape, frequency, and cantilever displacement was successfully collected and processed. It was found in the process of denoising that the application of the butterworth filter required that the data be slightly offset from the original in order to be sufficiently smoothed. Fortunately, the Butterworth filter preserves information of magnitude and frequency, which are the most relevant aspects of the data, and thus it was determined that the filter was sufficient for the purposes of analysis (Figure 12). Notably, the filtered data still retained a nontrivial oscillation visible in the low-voltage range. This oscillation is thought to arise from the mechanical motion of the test bed, and poses no obstacle to analysis – the oscillation's magnitude is largely negligible (on the order of 10^{-2} times smaller than the primary signal), and will not adversely affect calculations of energy or average power.

After processing, the voltage measurements were used alongside the known circuit resistance value of 220 kΩ to calculate power at each time step, which in turn was used to determine peak power output and total average power over time (Figure 13).

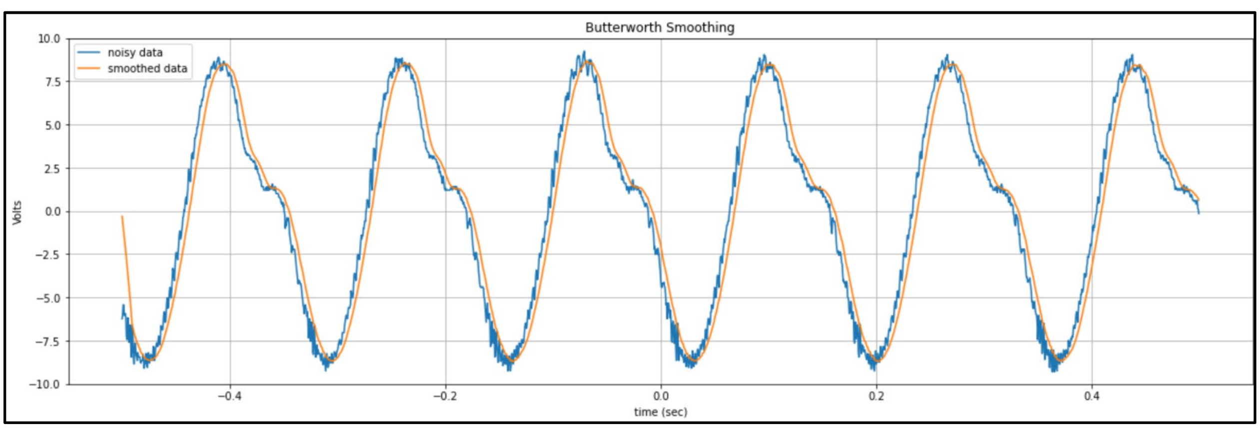

Figure 12: Comparison of raw data against the same data processed with a Butterworth Filter. Note the slight phase difference.

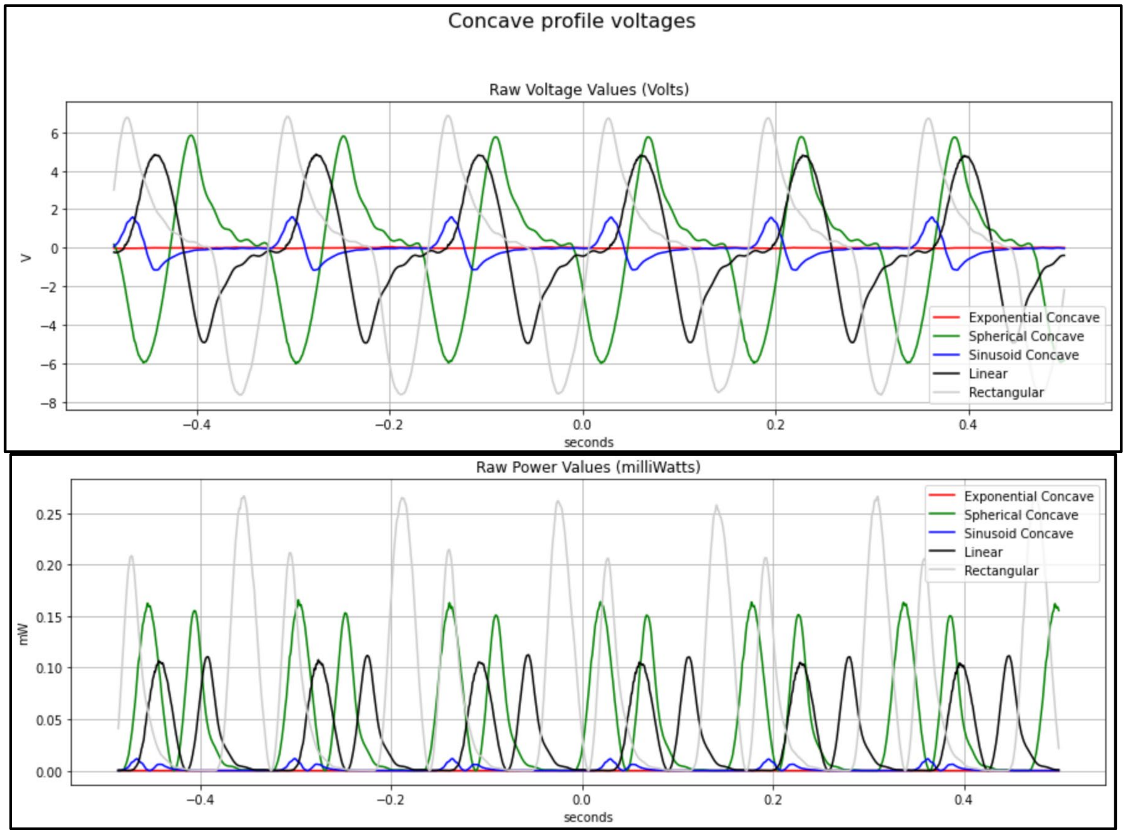

Figure 13: Processed data of concave cantilever voltage over time at 6Hz and 2mm displacement (above) against the calculated power in milliWattsfor each profile (below).

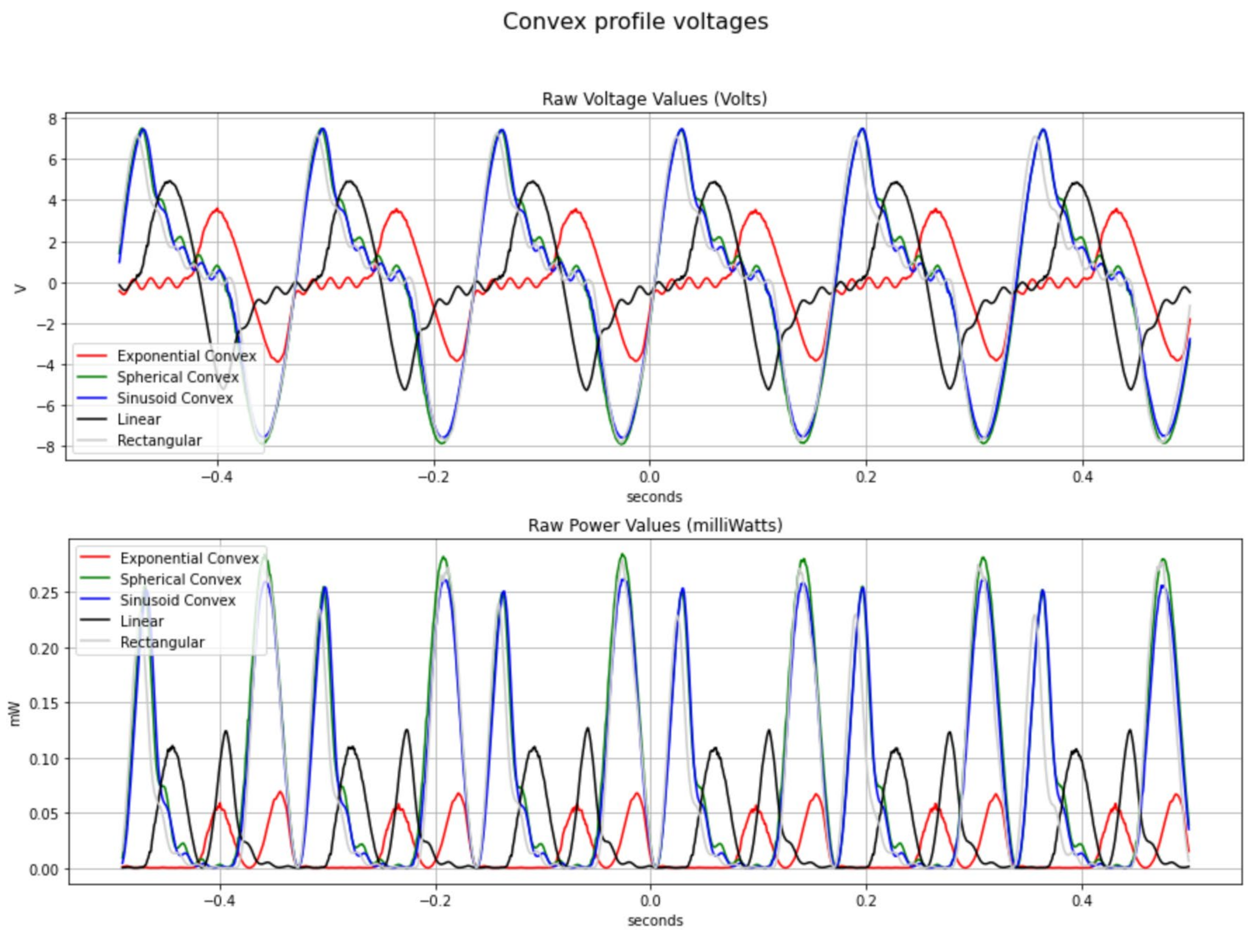

Figure 14: Processed data of convex cantilever voltage over time at 6Hz and 2mm displacement (above) against the calculated power in milliWattsfor each profile (below).

This data forms a reasonable basis for our findings, but is certainly different from how data would exist in a practical context. In contrast to our fairly smooth voltage variations, direct input from pedestrians would result in graphs which, while comparable in relative magnitude, would be less consistent in time and repetition. The rolling cylinder's impact is shorter than that of a footstep and has a force direction normal to the cantilever, whereas a footstep would have different force vectors during different points of the step. Additionally, in a practical context, we would see two major impacts per footstep: one when the foot first lands and one when it pushes back off the ground, each with their own force vector. This would cause the torque applied to the cantilever to act slightly differently and at a different, but scaled, magnitude. However, the idealized environment does not minimize the comparisons of voltage and resulting analysis of power between geometries for piezoelectric tiles. Additionally, the mechanism for striking the piezoelectric behaves differently than a real-world impulse from a foot. The duration for the force was much shorter than in real life, and the forces would not be nearly as regular or consistent as the test.

Chapter 5: Analysis

5.1: Cantilever Geometry Comparison

After analysis of the features of each of our data sets, we computed the peak and average power values of each of the differing geometries and compared them. The peak power and average power for each geometry was compared for unmodified values, and then for their value normalized by the piezoelectric areas determined in Chapter 4.1.

Our peak power values, shown in Figure 14, show that the spherical convex and sinusoidal convex designs exceed the rectangular shape for this parameter despite containing less piezoelectric material. Additionally, the spherical concave design also shows well above expected peak power for its cut, exceeding the power output of the linear design but failing to exceed the output of the rectangular design. Meanwhile, the exponential concave, sinusoidal convex, and exponential convex designs all perform at lower power than both control designs of linear and rectangular. These notions are reinforced by the area normalized analysis of Figure 15, showing that outputs of the spherical and sinusoidal convex are roughly equivalent.

This indicates the action of a more optimal strain distribution exploited in these particular shapes, which would focus the distortion of the cantilever at a single focal point near the fulcrum. The spherical convex and sinusoidal convex cantilevers in particular are able to exceed the output of either basic cantilever geometry, leading to the possibility that these are more optimal geometries than conventional piezoelectric cantilevers.

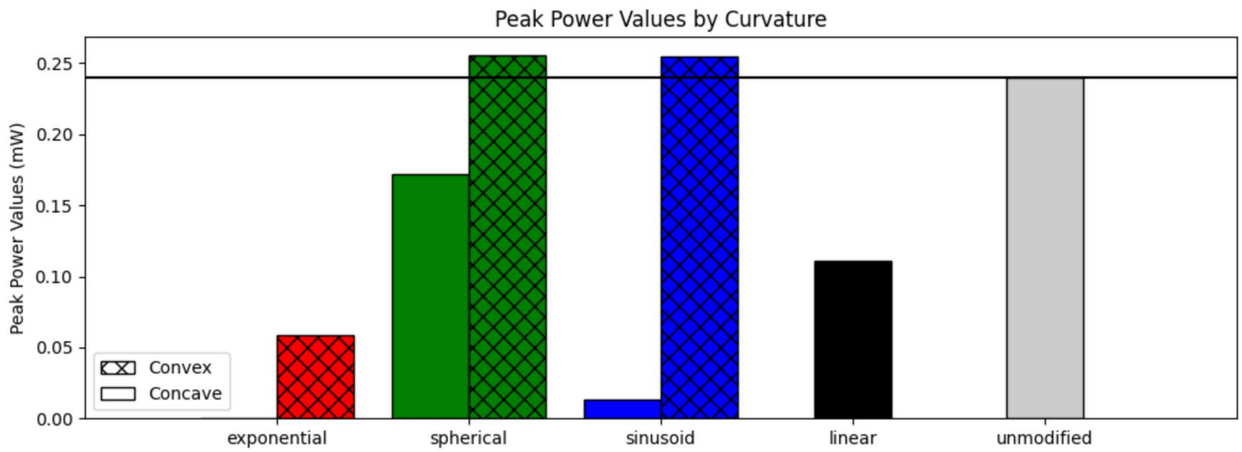

Figure 15: Peak Values of Each Piezoelectric Cantilever Curvature

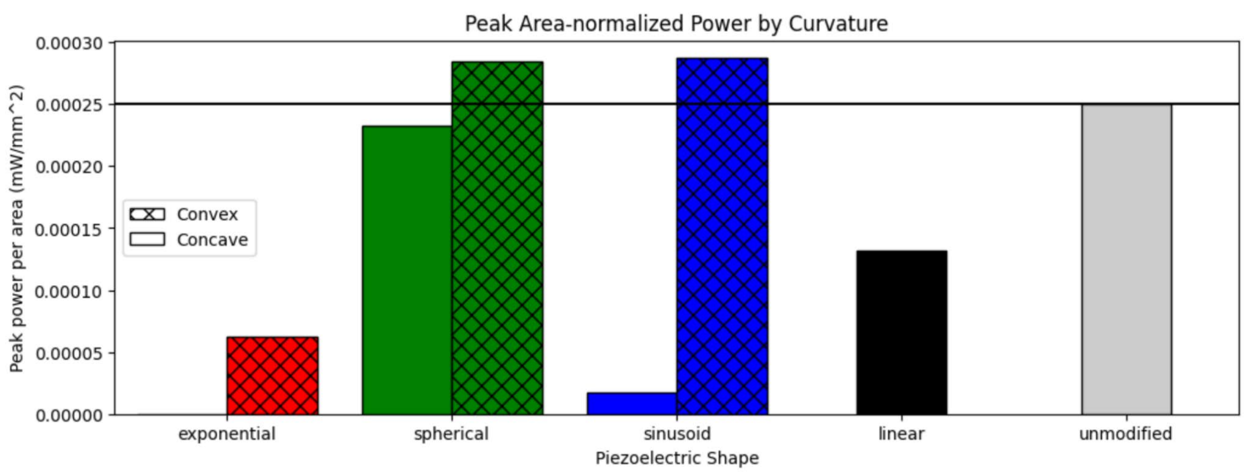

Figure 16: Peak Values of Each Piezoelectric Cantilever Curvature, Area-Normalized

Analysis of the average power over one-second intervals reveals a similar pattern. For both the standard and area normalized analyses in Figure 17 and Figure 18, the same relationships arise with the exception of a more apparent difference in the power output of the spherical convex and sinusoidal convex: This suggests the spherical concave cantilever profile produces wider voltage peaks. Numerical analysis indicates the spherical convex design is the most effective by a significant margin, producing 124 percent the power of the unmodified rectangular piezo.

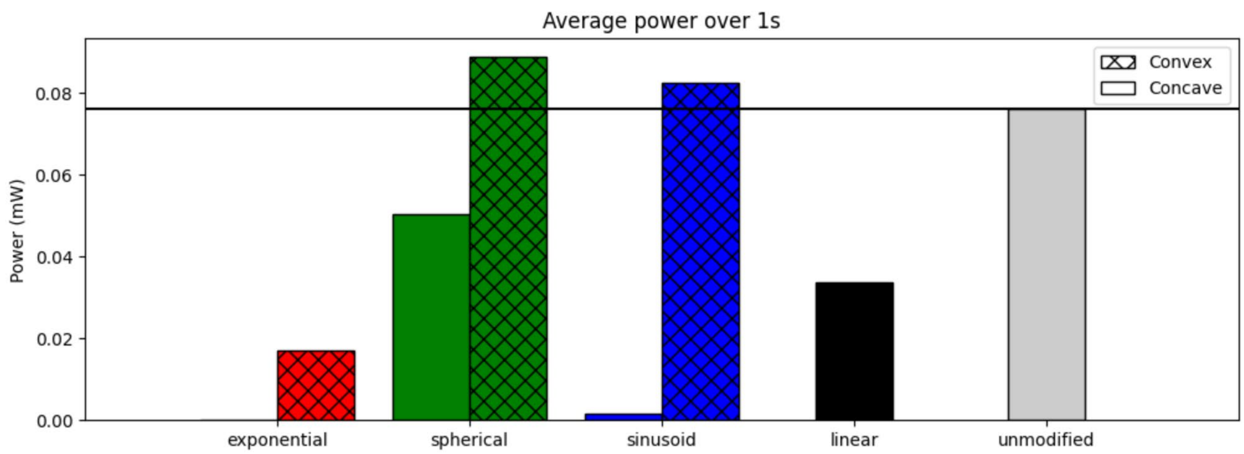

Figure 17: Average Power Output of Each Piezoelectric Cantilever Curvature

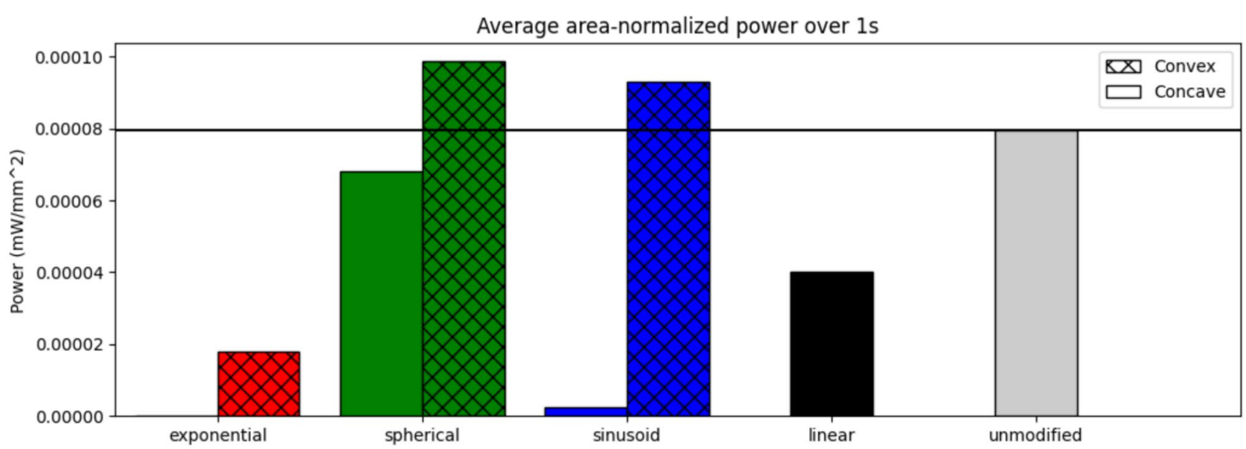

Figure 18: Average Power Output of Each Piezoelectric Cantilever Curvature, Area-Normalized

Cantilever	Percent Power Output of Rectangular
Exponential Concave	0%
Spherical Concave	85.65%
Sinusoidal Concave	2.88%
Exponential Convex	22.70%
Spherical Convex	124.37%
Sinusoidal Convex	117.37%
Linear Taper	50.57%

Figure 19: Ratio of Modified and Unmodified Power Outputs.

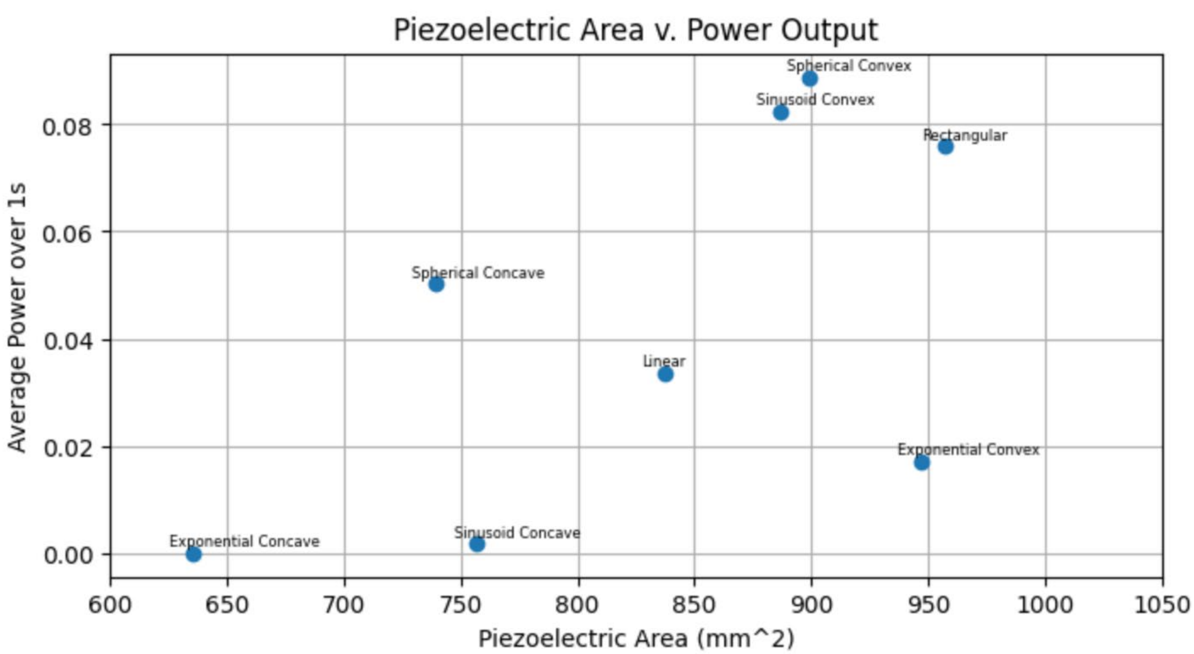

Figure 20: Piezoelectric Area vs Average Power for each Curvature

5.2: Internal Resistance Measurement

The variable resistance measurements were collected and smoothed with the same method outlined above, and the peak-to-peak voltage maximum of each resistance value was measured as a consistent point by which the Thevenin resistance can be calculated. The applied load was graphed against the associated peak voltage, as shown in figure 21.

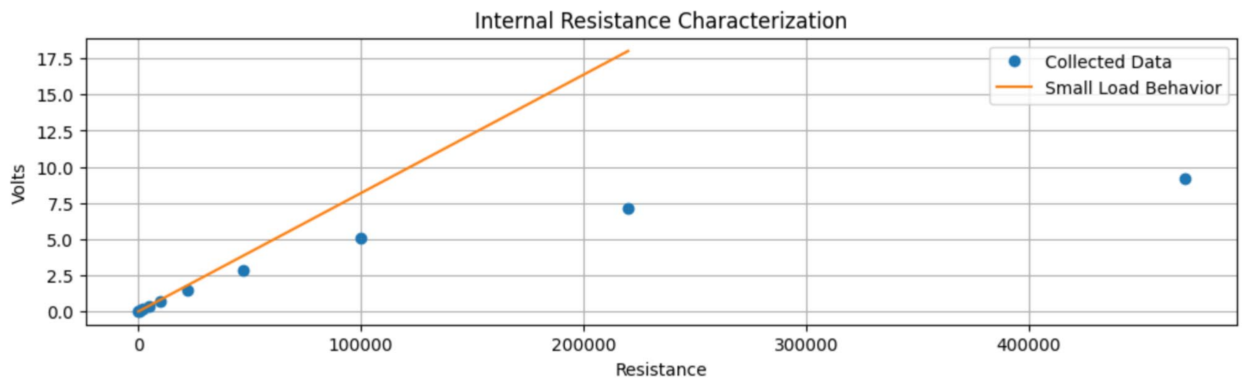

Figure 21: Load resistance for the peak value of a rectangular cantilever driven at 6Hz with 2mm displacement. The small load behavior line has slope I_{sc}, the short circuit current.

Taking the slope between the two data points of lowest load where a voltage peak was still discernible produces a calculation for the short circuit current $I_{sc} = 8.18 * 10^{-5}$ amperes, which was then applied to Ohm's law alongside the measured open circuit voltage to estimate the internal resistance of one unmodified cantilever:

$$\frac{V_{open}}{I_{sc}} = \frac{10.77}{8.18 * 10^{-5}} = 131627\ Ohms$$

This value of 131 kΩ aligns with expectations based on the insulative nature of PZT, which is a ceramic material. The metric indicates that an application of this method is best applied at scale, across a large surface containing a multitude of PZT cantilevers wired in parallel. In order to match the internal resistance of a common battery, for example, 146,000 of these cantilevers would need to be wired together, for a total of 140 square meters of piezoelectric. Keeping in mind that a surface does not have to be plated in piezoelectric to achieve such a goal, and that the cantilevers would be spread across a comparatively large area, this suggests a very large floor space required to effectively implement this technology.

This metric allows piezoelectric energy harvesting to be immediately viable in areas of large floor space and high traffic, such as building atriums, but restricts its effective use in smaller areas such as corridors or public transit stations. Further development into low-resistance options for such an application would allow for more varied options.

Chapter 6: Discussion

6.1: Comparison to Existing Literature

Pradeesh et Al, as previously reviewed, places an emphasis on the efficiencies associated with linearly tapered shape. In that publication, inverted tapered cantilevers were manufactured and affixed with sheets of PZT ceramic on their surface. The resulting harvesters demonstrated a dramatic amplification of p-p voltage when the cantilever was inversely tapered in width, and even more so when the tapered in both width and thickness. [41]

Notably, the linear cantilever in this study demonstrated a marked decrease in voltage output: the inversely-tapered linear profile produced only 50.57% of unmodified voltage output, in apparent contradiction to the above paper. This is likely due to differences in methodology regarding the manufacture and positioning of the piezoelectric: While *Pradeesh et al* produced their own cantilevers of solid aluminum and affixed a piezoelectric element to its surface, this paper used premade piezoelectric transducers cut to shape, which removes some of the embedded piezoelectric element. Considering that the majority of the material removed to produce an inverted taper is located at the base of the cantilever, this may explain the discrepancy. In addition, the manufacturing process for these tapers has been known to damage the piezoelectric on occasion, as can be seen by the performance of the exponential convex curve. It is possible that this has also occurred in the linear cantilever: a hairline fracture may be the culprit behind halving the linear taper's performance.

Nonetheless, the performance of the convex cantilevers supports the assertions drawn from existing literature. Prior publications discussed the correlation between the shape and peak power of the cantilever, and suggests that inverted tapers produce higher power outputs compared to their regularly tapered counterparts, showing increased power outputs as high as 45%. Comparing this existing literature to our study, supports the conclusion that the concave and convex spherical shapes, which can be compared to prior knowledge, exhibit increased peak-to-peak voltage. This suggests the need for future research into this amplification method.

6.2: Future Research Potential

As per our analysis, altering the shape of the piezoelectric cantilever does, in fact, have the potential to impact the power output of the cantilever. Moreover, since our cantilevers were all cut from a controlled rectangular shape and the cuts resulted in both positive and negative differences in power output, there is clearly an optimum to be found. One avenue of further research touches on the investigation of more shapes to discover said optimum. This definition of optimum changes based on the required application. For our potential future investigation of piezoelectrics in floor tiles, we would need to be maximizing power output and durability, while minimizing the surface area and cost of the cantilever.

In addition, we would want to ensure that further testing works to improve upon some of the drawbacks that we encountered during our experimentation. For instance, we would want to find a safer means of creating curvatures to test with. As mentioned, we used a subtractive process of waterjet cutting to take an uncut piezo wafer and shape it into our desired curvatures, but this left room for potential damage. One idea to remedy this issue is to have the cantilevers custom made by a third party so as to eliminate the risk of damage. Moreover, while we tested our cantilevers in low frequency environments, we hypothesize that the output of the cantilevers would be higher closer to their respective resonance frequencies. Our cantilevers were tested at approximate footstep frequencies and not at specific resonance frequencies of the material. As such, in future testing, we would want to take the preliminary step of empirically determining the resonance frequencies of the cantilevers being tested. We could then use the resonance frequencies of the cantilevers as the baseline frequency and observe how the output of the cantilevers change as we move the testing frequency away from its resonance frequency.

Another avenue of research to consider is that of magnetic amplification. While it was not a path that was explored by PISO, we did discover through our literature review that the use of magnets can have a positive effect on the energy harvesting capabilities of piezoelectric cantilevers. Moreover, there have been prototypes of piezoelectric floor tiles that have implemented magnets. This use is something we strive to further show to be useful and feasible using varyingly shaped cantilevers, so as to add to our current results.

While PISO has added to the field of knowledge in piezoelectric energy harvesting, there are still steps that need to be taken to design a fully optimized piezoelectric tile. Our project has observed the power output of varied cantilever shapes, but there are other factors that need to be considered. Namely, information such as energy yield, energy lost to nonconservative forces, the damping effect of hysteresis, the maximum acceptable “give” of the tile, durability of the tile, pedestrian traffic patterns, and the significance of Curie’s Law will all need to be considered, just to name a few. Clearly, this leaves a lot of work carved out. As such, it constitutes another avenue of further research. The investigation of each of these factors independently would need to be completed prior to the investigation of all of them together.

6.3: Final Thoughts

This paper outlines the results of an investigation into the effect of a cantilever’s shape on its strain distribution, and by extension its effectiveness as a piezoelectric energy harvester. Eight cantilevers were tested: One unmodified rectangle, one outwards taper, and six more curved outwards tapers following spherical, sinusoidal, and exponential curves. For each of the three curves, a concave and convex variant were produced. Each of these cantilevers was tested under a range of displacement and frequency values by applying discrete impulses to it using an adjustable camshaft, and the resulting voltages were analyzed and compared.

Of the seven modified cantilevers produced, two were notable for having a higher output: The convex spherical and convex sinusoidal curves. These curves amplified the average power output of the cantilever by a factor of 124% and 117%, respectively, significantly increasing power even while portions of the piezoelectric element were cut away in the manufacturing process. Notably, these spherical and sinusoidal curves were the most similar to one another in shape among the tapers tested, suggesting the involvement of some mechanical or electrical phenomenon which arises in a certain character of tapered cantilevers.

The results outlined in this paper are not conclusive. The sample size for each type of taper was limited by the availability of manufacturing equipment, and damage to the piezoelectrics during manufacturing prevented full exploration of the capabilities of all seven tapers. Nonetheless, the pattern suggested by the boosted performance of two similarly-shaped curved cantilevers indicates there may be an opportunity for further research in this vein. Research into the maximally-amplifying curve profile for a piezoelectric cantilever would not only allow for more efficient energy harvesting, but would also produce more sensitive piezoelectric sensors and actuators.

Appendices

Appendix A: Glossary

Arctic Amplification - the phenomenon that occurs due to the excess of carbon dioxide in the atmosphere; any change in the planet's net temperature balance will have a pronounced effect in the poles

British thermal unit - a unit of heat, formally defined as the amount of heat needed to increase the temperature of a single pound of water by one degree fahrenheit

Coupling Mode - a method of examining the interconnectedness of vibrational systems, either mechanical, electrical, or more, within time or space

Intermittency - is capable of stopping for certain periods of time and then alternately ceasing and starting once again

Dynamo - an electrical generator that utilizes electromagnetism in order to create direct current

Magnetic Induction - the creation of voltage in an electrical conductor within a magnetic field

Perovskite Structure - A crystal with a similar crystalline structure to $CaTiO_3$, also known as Perovskite

Piezoelectric Charge Coefficient - The conversion rate between newtons of force to coulombs of charge

Photovoltaic Cells - also known as a solar cell, a device that transforms solar energy, or the energy from light, into electrical energy utilizing the photovoltaic effect

Piezoelectric Effect - the ability of piezoelectric materials to create electricity due to mechanical stress

Poling Direction - The direction of positive polarization in a piezoelectric material

Appendix B: Budget

The following table details the purchases made for the experimentation and construction completed throughout the course of Team PISO's research. Acquisition of monetary funds through grants, awards, and fundraising efforts are noted chronologically in Appendix C: Timeline.

Material	Price	Quantity	Purchase Date	Expenditure
Piezoelectric Bending Transducer	$133.10	5	2021-10-02	$665.50
Locking Positioning Tables with Micrometer	$435.00	1	2021-10-26	$435.00
Ball Bearings	$6.25	2	2021-10-26	$12.50
18-8 Stainless Steel Button Head Hex Drive Screw (1/4"-20 Thread Size, 1-1/4" Long)	$5.48	1	2021-10-26	$5.48
18-8 Stainless Steel Button Head Hex Drive Screws (1/4"-20 Thread Size, 1/2" Long)	$5.57	1	2021-10-26	$5.57
18-8 Stainless Steel Button Head Hex Drive Screw (1/4"-20 Thread Size, 3/4" Long)	$6.95	1	2021-10-26	$6.95
Black-Oxide Alloy Steel Socket Head Screw (0-80 Thread Size, 7/8" Long)	$13.64	1	2021-10-26	$13.64
18-8 Stainless Steel Dowel Pin	$13.52	1	2021-11-05	$13.52
Positioning Table with Micrometer (Locking, 30 lbs. Static Load Capacity)	$438.67	1	2021-12-07	$438.67
Black-Oxide Alloy Steel Socket Head Screw (10-32 Thread Size, 1/2" Long)	$13.17	1	2022-02-17	$13.17

Roller Chain, 2ft	$9.28	1	2022-03-08	$9.28
Connecting Link for Single Strand Roller Chain	$0.95	10	2022-03-08	$9.50
Aluminum Flanged Screw-to-Expand Insert	$9.42	1	2022-03-08	$9.42
10:1 Metal Gearmotor 37Dx65L mm 12V with 64 CPR Encoder (Helical Pinion)	$39.95	1	2022-03-08	$39.95
Arduino Uno Rev3	$23.00	3	2022-04-21	$69.00
Piezoelectric Bending Transducer	$266.20	10	2022-11-03	$2,662.00
Charger Connector 12v	$20.99	2	2023-02-14	41.98
Ni-MH Rechargeable Battery 12V 2000mAh	$21.68	1	2023-02-14	$21.68
Total				**$4472.81**

Appendix C: Timeline

Spring 2020:

- Team PISO officially formed through the Gemstone Honors Program at the University of Maryland (UMD)
- The following UMD faculty assigned as university resources for the research team:
  - Mr. Rick Blanton, *Director of Technical Operations for the A. James Clark School of Engineering*
  - Ms. Nevenka Zdravskovska, *Head of the STEM Library*
- Began biweekly online meetings with the team, and with team mentor Rick Blanton due to COVID-19 pandemic

Fall 2020:

- Applied for and obtained the Maryland Sea Grant (awards NA14OAR4170090 and NA18OAR4170070) from National Oceanic and Atmospheric Administration, U.S. Department of Commerce

Spring 2021:

- Unable to conduct in-person testing due to Covid-19 pandemic, so started to construct experiment plans and make a plan for ordering materials, and brushed up on matlab skills for simulation preparation
- Participated in lab training in anticipation of apparatus construction
- Proposed thesis on February 24, 2021 online with the following UMD faculty in attendance:
  - Mr. Rick Blanton, *Team PISO Mentor*
  - Dr. Romel Gomez, *Professor of Electrical and Computer Engineering*

  - Dr. David J. Lovell, *Director of the Gemstone Honors Program*
  - Dr. Kristan Skendall, *former Associate Director of the Gemstone Honors Program*

- LaunchUMD Giving Day on March 3, 2021; raised $5,450 in our campaign as well as an extra $500 for reaching 100 donors, and $250 for receiving the most donations that day (from LaunchUMD)
- Received $5000 from the University Sustainability Council in a Sustainability Fund Grant on March 5, 2021

Autumn 2021:

- Commencement of in-person meetings and discussions as Covid-19 restrictions at UMD began to subside
- Explored experimentation plans and test rig concepts, settled on first test apparatus
- Modeled and printed main components, as well as ordered the required materials for construction of the first testing apparatus
- Presented at the Do-Good Showcase; won the Panelist's Award of $500 from the Do Good Institute for our presentation on social impact

Spring 2022:

- Presented a team poster detailing our progress at Undergraduate Research Day on April 27, 2022

Autumn 2022:

- Piezoelectric component manufacture
- Data collection with custom curvatures
- Data analysis code development.

Spring 2023:

- Finalizing data analysis
- Thesis conference on April 14, 2023 with the following discussants in attendance:
    - Mr. Rick Blanton, *Team PISO Mentor*
    - Dr. Xi Chen, *Postdoctoral Researcher, Department of Electrical Engineering and Materials Science and Engineering, Materials Research Institute, The Pennsylvania State University*
    - Dr. John Cumings, *Professor of Materials Science and Engineering, UMD*
    - Dr. Romel Gomez, *Professor of Electrical and Computer Engineering, UMD*
    - Dr. Isabel Lloyd, *Undergraduate Program Director of Materials Science and Engineering, UMD*
    - Dr. David J. Lovell, *Director of the Gemstone Honors Program*
- Citation ceremony on May 17, 2023, marking the completion of the Gemstone Honors Program

Appendix D: Equity-Impact Analysis

Team PISO's research and the significance of identifying a more efficient method of collecting energy extends past its potential environmental effects. Such discoveries would affect societies and economies as a whole through accessibility, and by extension, the price of energy. Ideally, the optimization of piezoelectric energy generation would make energy cheaper for those living wherever piezoelectric tiles are put into practice, and thus will indirectly benefit people of the lower class by reducing their expenses.

The concept of a piezoelectric floor tile also brings about a new dimension of societal impact due to its direct contact with the public. The nature of such a design requires the interaction of pedestrians, requiring the consideration of accessibility, comfort, and durability. Depending on the requirements of a specific piezoelectric tile design and the implementation of that technology, the terrain underfoot created by the tiles may be more malleable than wood, stone, or concrete. This would affect people using wheeled vehicles, such as wheelchairs, bikes or powered scooters, by making the terrain slightly harder to cross. However, it must be noted that this impact is dependent on many conditions which can be compensated for, and is thus avoidable.

It is essential for the guidelines set by The Americans with Disabilities Act (ADA) to be integrated in the design considerations of any piezoelectric tiles. ADA laws specify the required distance between floor tiles and the maximum amount of elevation between levels to ensure accessibility for various forms of transportation. While these restrictions may be relevant towards the actual production of implementable tiles, as we have investigated the optimization of the shape of piezoelectric ceramics inside of them, thickness of the piezoelectric component tile seems to have a minimal effect on the full size of the tile.

Additionally, piezoelectric tiles can be an incentive to encourage walkable urbanism, which is measured by the amount of errands that can be accomplished on foot. The prospect of a publicly available method of generating electricity for the community using pressure that would be generated anyway by pedestrians would be a source of motivation for those living in the affected areas to walk more. Walkable urbanism, while improving public health and decreasing the amount of pollution generated by other modes of transportation, is also correlated with higher per-capita GDPs. According to an analysis conducted by George Washington University, encouraging walkable urbanism is a potential strategy for regional economic development. Hence, piezoelectric tiles can be an important factor in contributing towards economic development.

However, this support towards economic development also has the potential to bring about the displacement of lower-income areas as a consequence of the increasing land value. Thus, implementation of piezoelectric tiles in urban areas could lead to a higher rate of gentrification. This would disproportionately affect the resident lower-class population by raising rent prices beyond what some people can afford, requiring many of them to find a home elsewhere. Thus, widespread use of piezoelectric tiles could contribute to a rise in homelessness and a widening of the wealth gap.

It is important to note all potential effects of implementing this technology, including the negative consequences that are bound to occur, as keeping them in mind could allow us to proactively avoid them. That being said, because this technology is relatively new and not as popularized as other alternative forms of energy generation, the unknowns can seem to overshadow the existing literature. Through the research conducted by our team, we recognize the potential impacts of piezoelectric ceramics and the existence of a future society that can benefit from its properties with additional research and studies.

Appendix E: Additional Results

1. Exponential Concave

    a. Effects of varying displacement on voltage output for exponential concave.

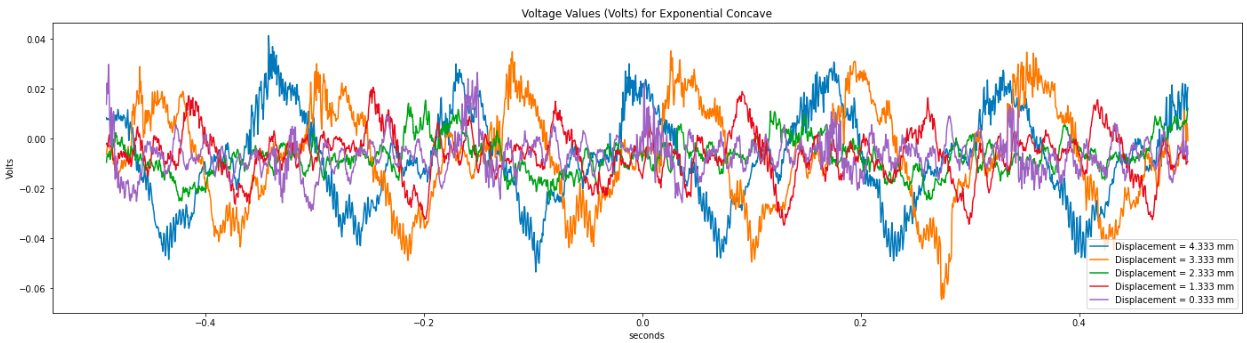

    b. Effects of varying displacement on power output for exponential concave.

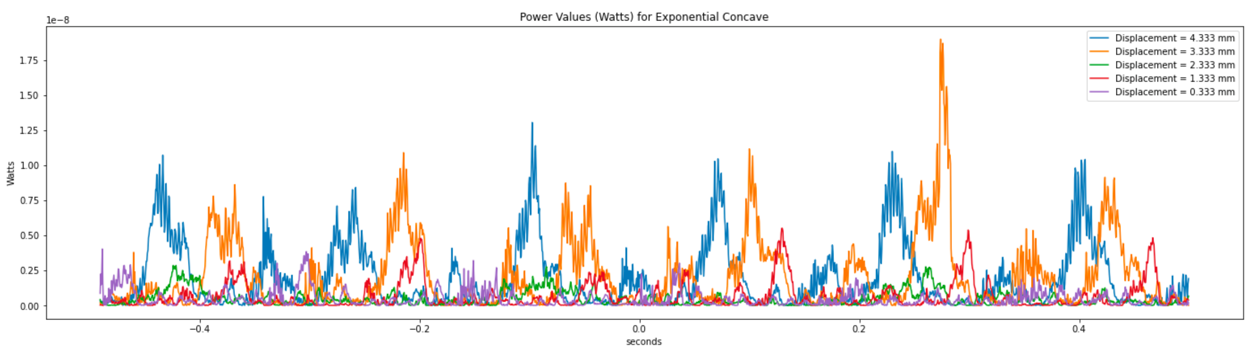

    c. Effects of varying frequency on voltage output for exponential concave.

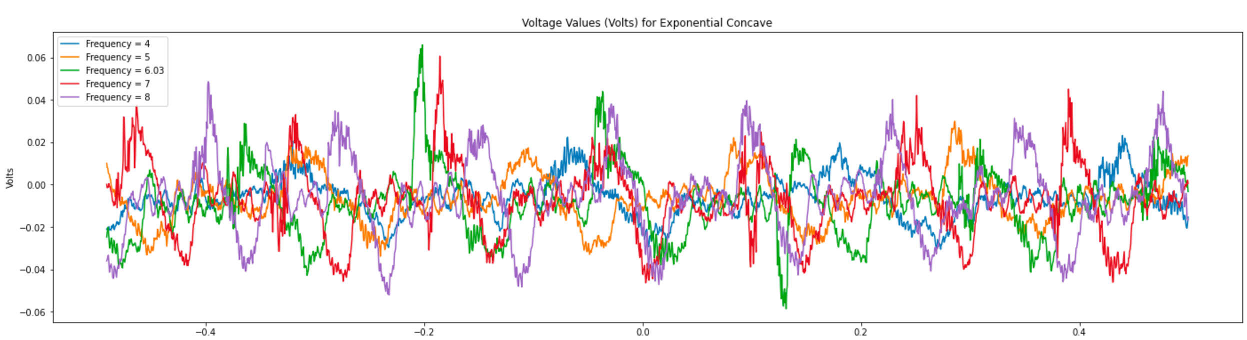

    d. Effects of varying frequency on power output for exponential concave.

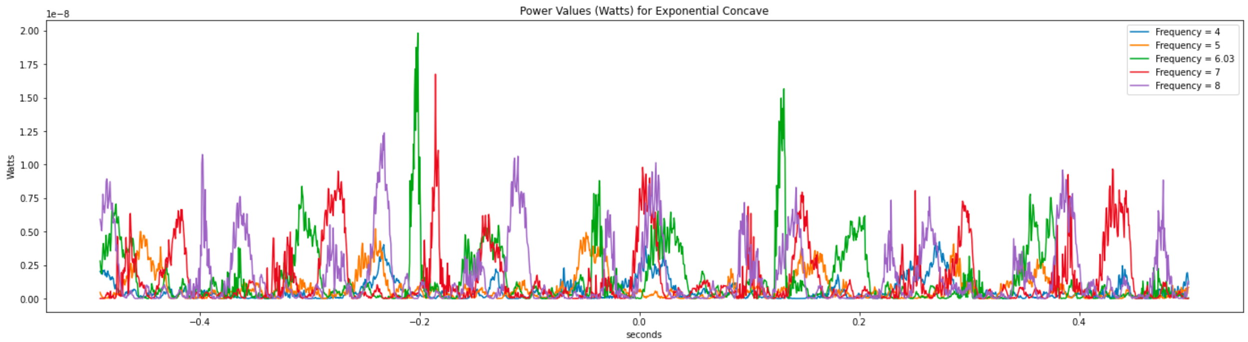

2. Exponential Convex

a. Effects of varying displacement on voltage output for exponential convex.

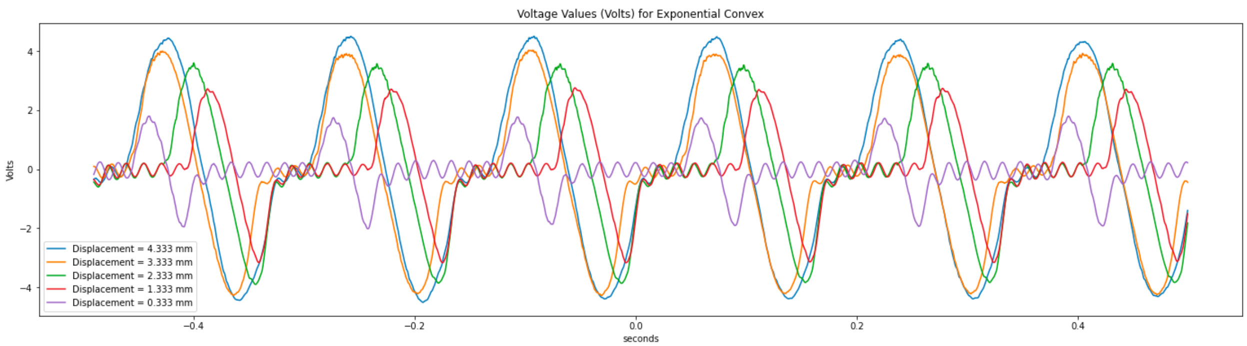

b. Effects of varying displacement on power output for exponential convex.

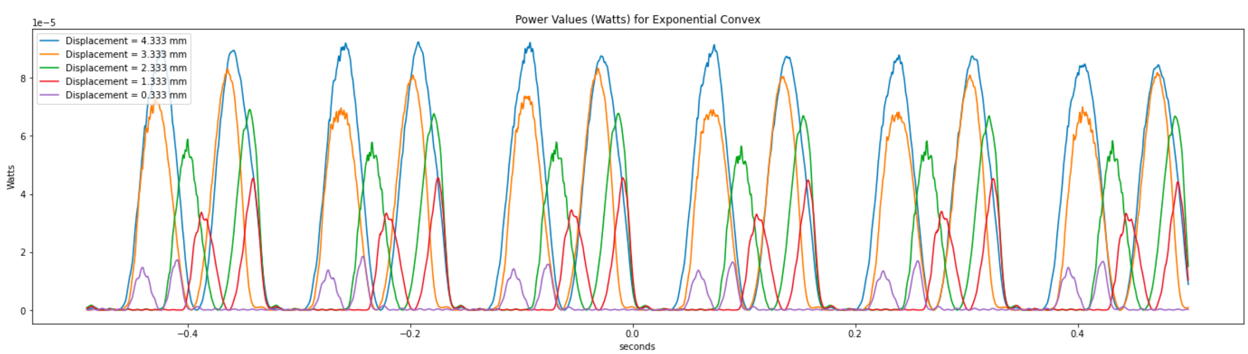

c. Effects of varying frequency on voltage output for exponential convex.

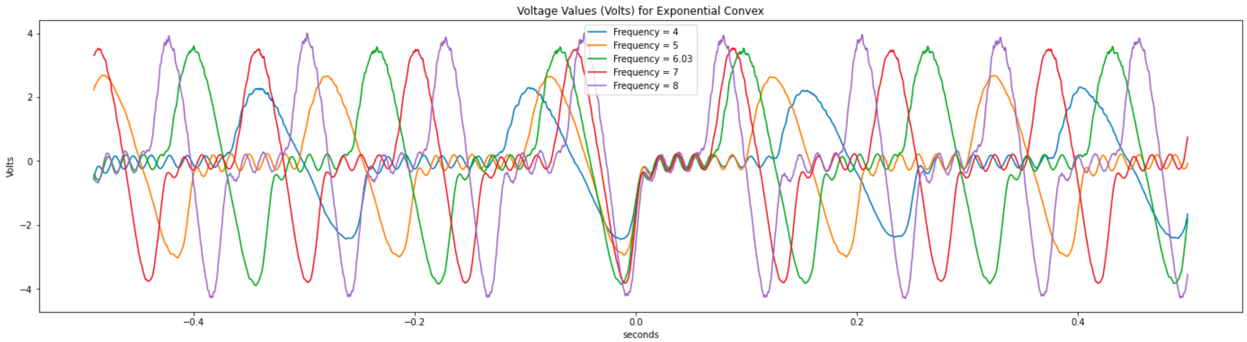

d. Effects of varying frequency on power output for exponential convex.

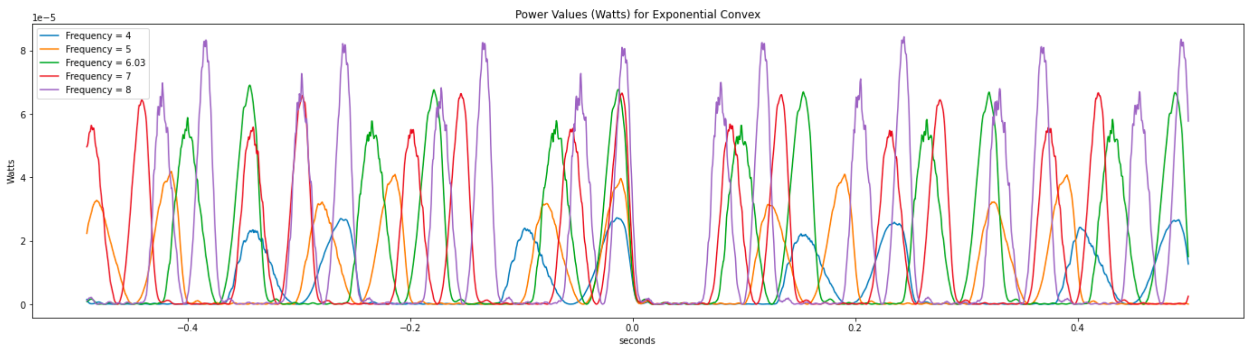

3. Spherical Concave

a. Effects of varying displacement on voltage output for spherical concave.

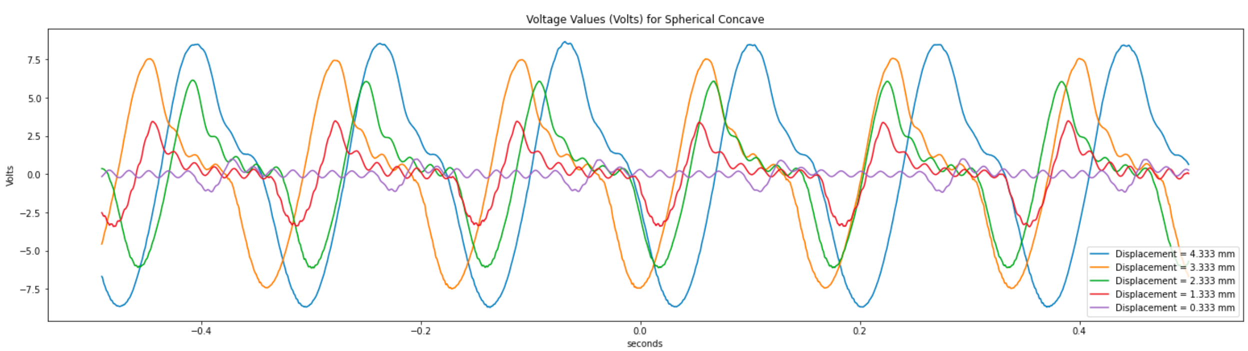

b. Effects of varying displacement on power output for spherical concave.

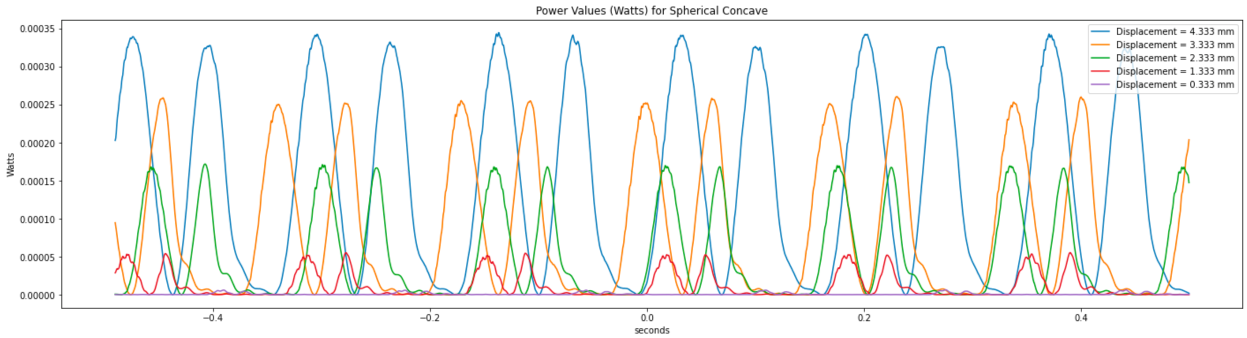

c. Effects of varying frequency on voltage output for spherical concave.

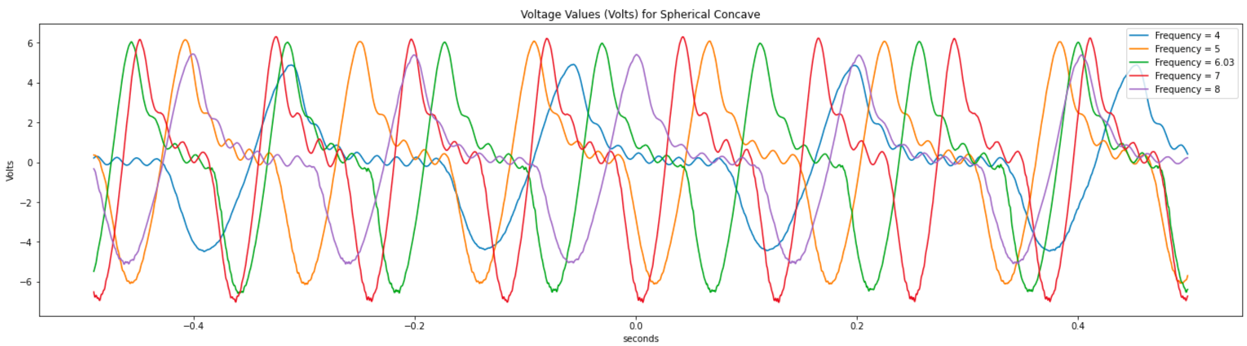

d. Effects of varying frequency on power output for spherical concave.

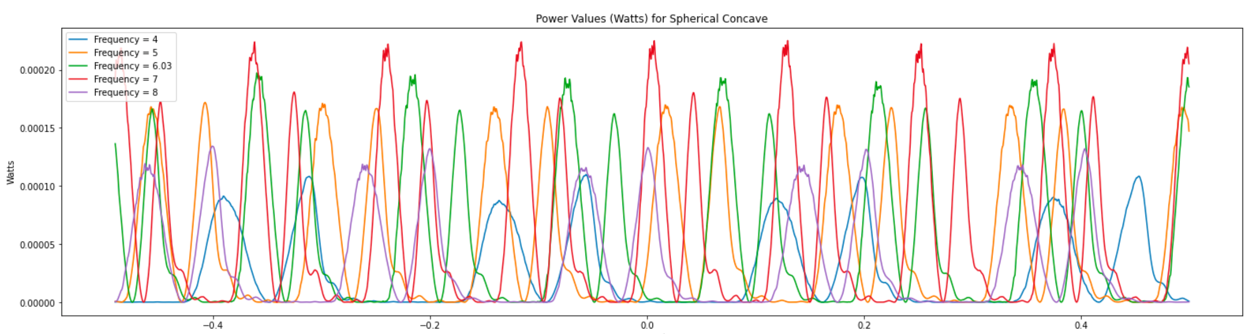

4. Spherical Convex

a. Effects of varying displacement on voltage output for spherical convex.

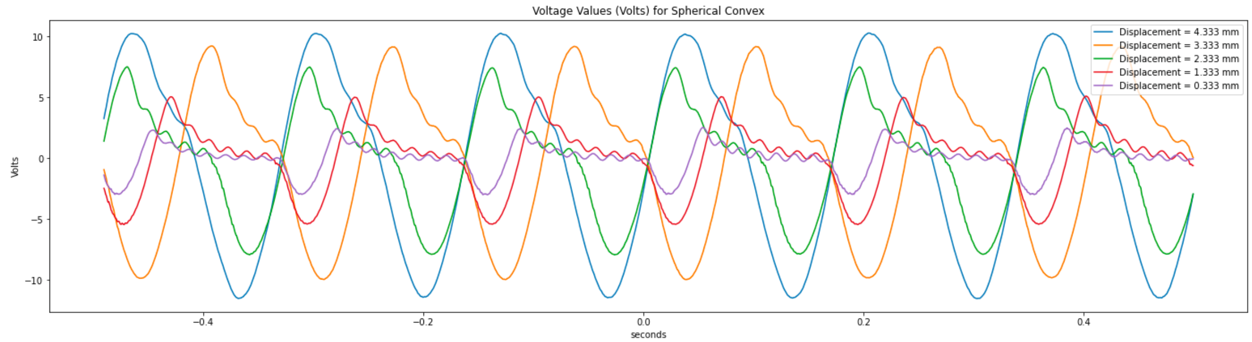

b. Effects of varying displacement on power output for spherical convex.

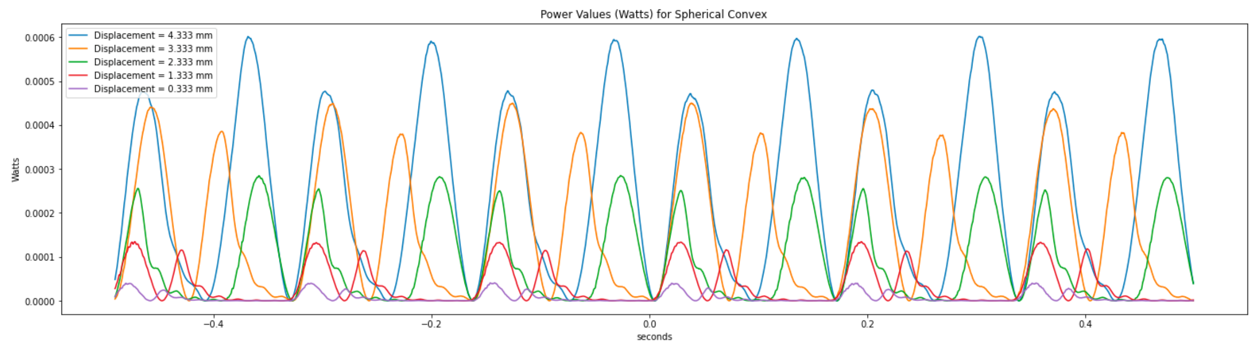

c. Effects of varying frequency on voltage output for spherical convex.

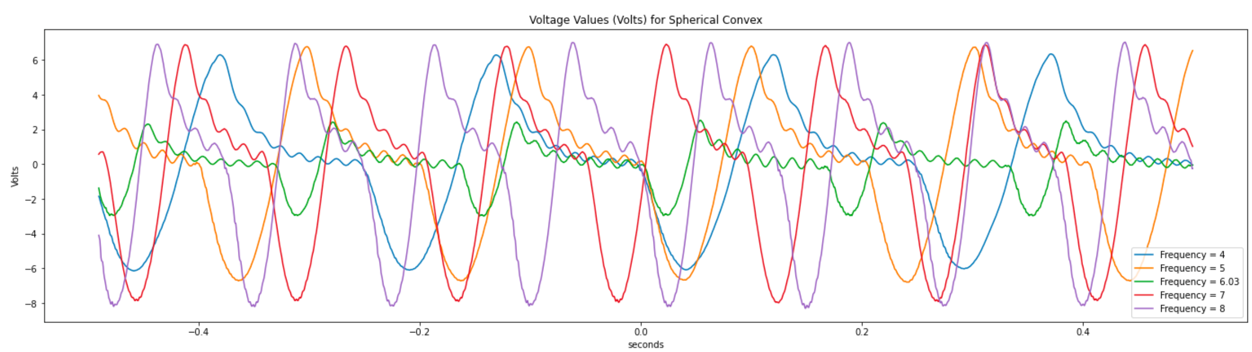

d. Effects of varying frequency on power output for spherical convex.

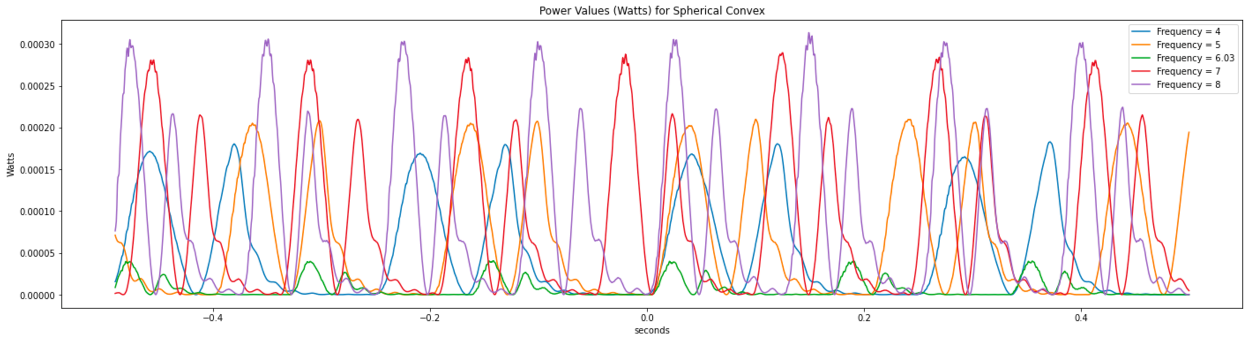

5. Sinusoid Concave

a. Effects of varying displacement on voltage output for sinusoid concave.

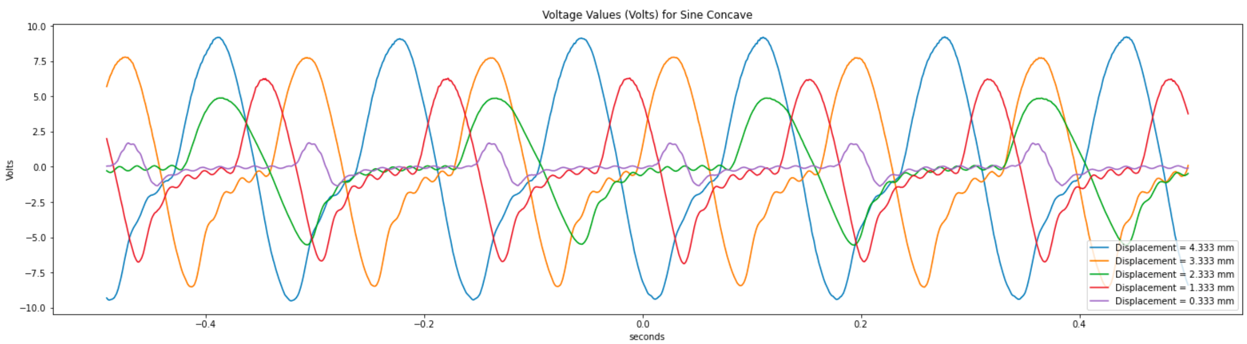

b. Effects of varying displacement on power output for sinusoid concave.

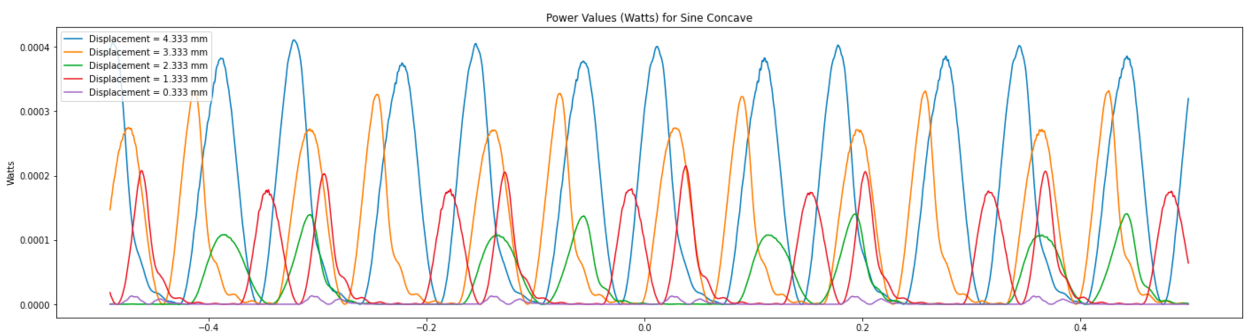

c. Effects of varying frequency on voltage output for sinusoid concave.

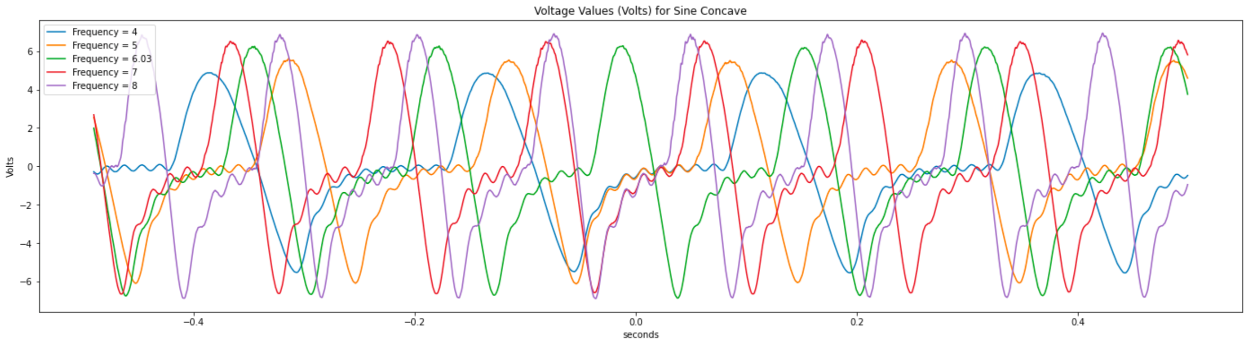

d. Effects of varying frequency on power output for sinusoid concave.

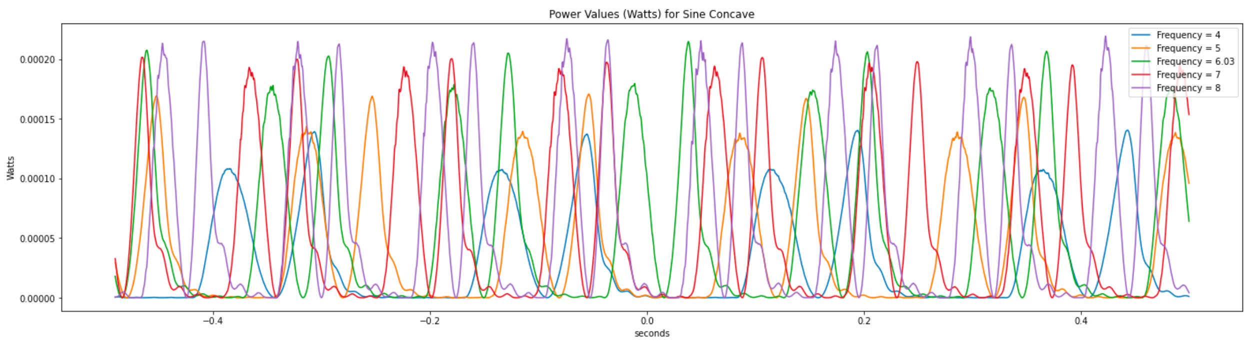

6. Sinusoid Convex

a. Effects of varying displacement on voltage output for sinusoid convex.

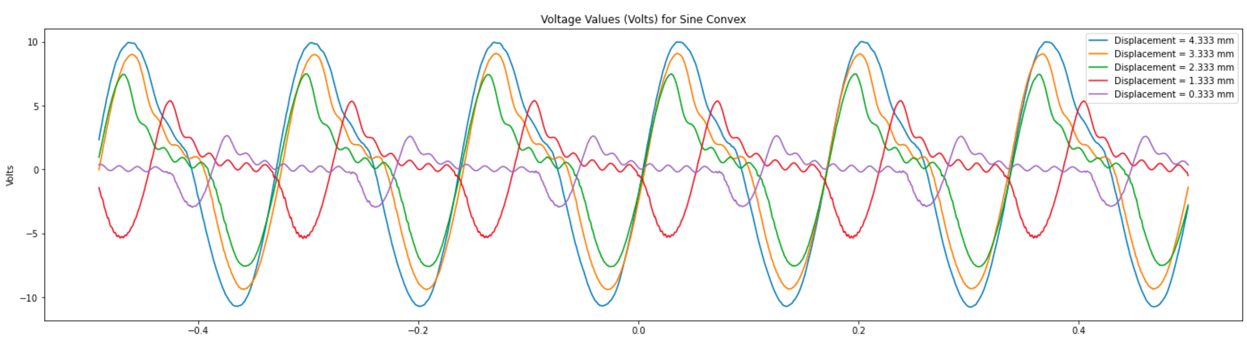

b. Effects of varying displacement on power output for sinusoid convex.

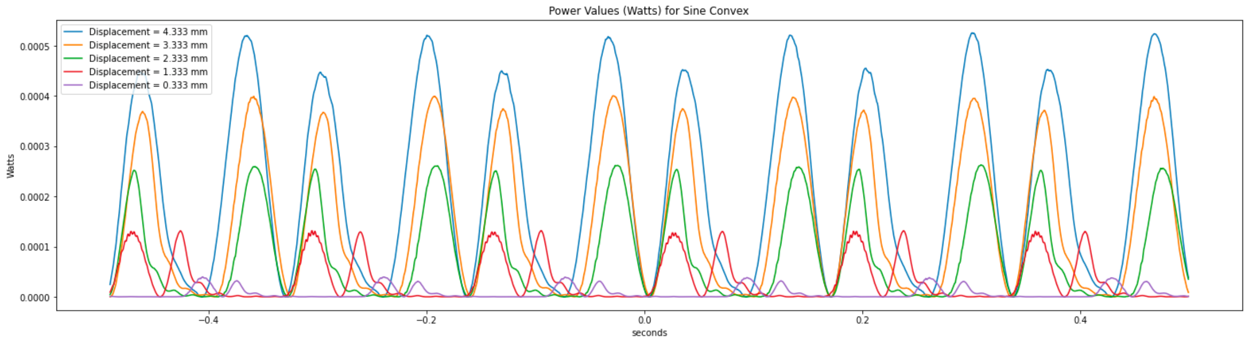

c. Effects of varying frequency on voltage output for sinusoid convex.

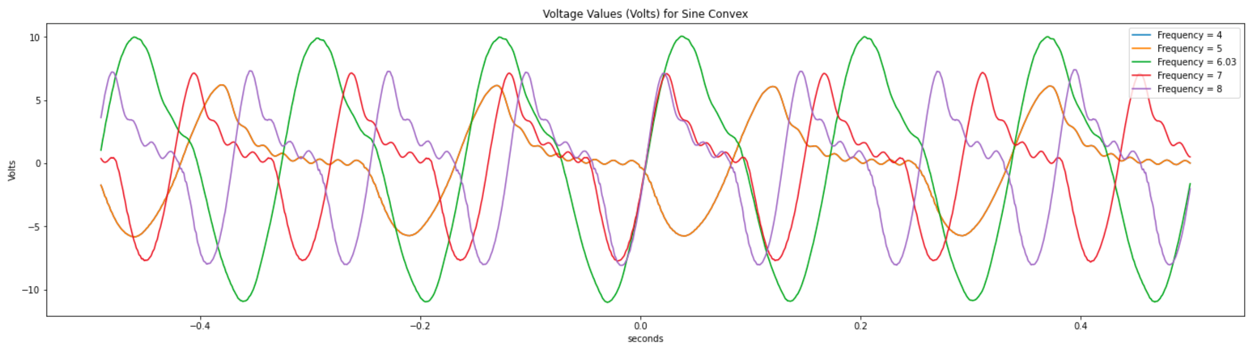

d. Effects of varying frequency on power output for sinusoid convex.

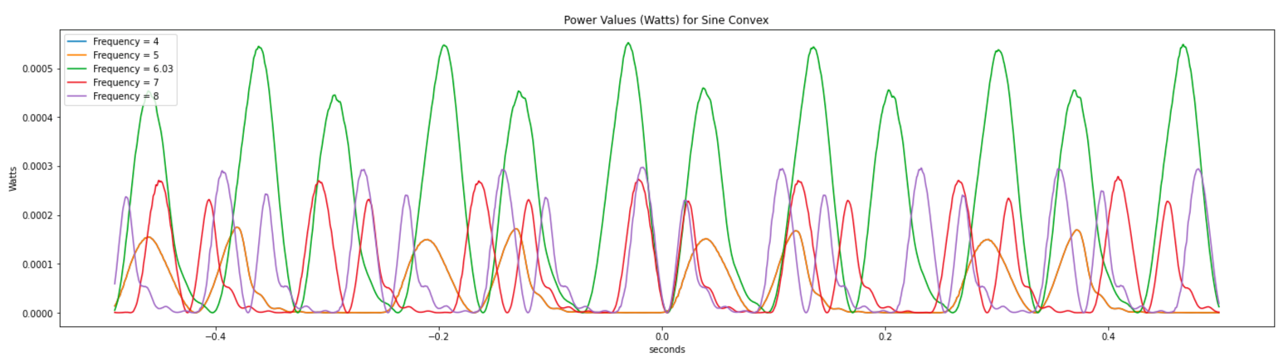

7. Linear

a. Effects of varying displacement on voltage output for linear.

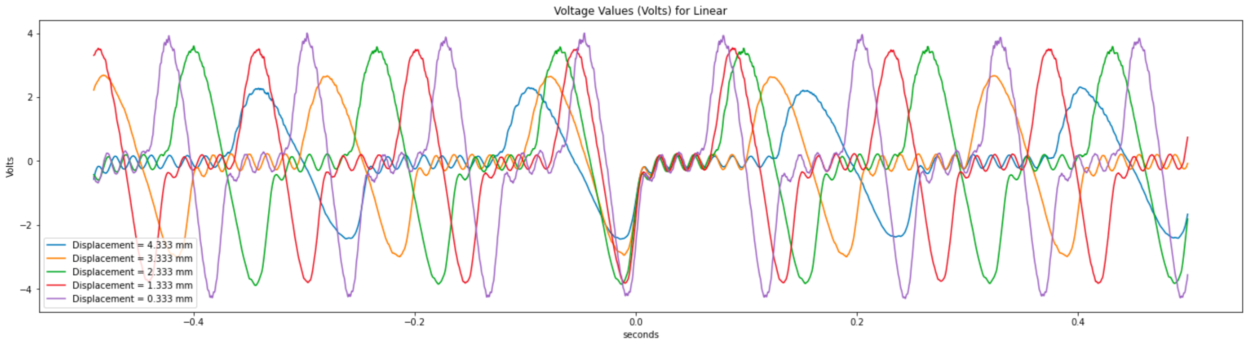

b. Effects of varying displacement on power output for linear.

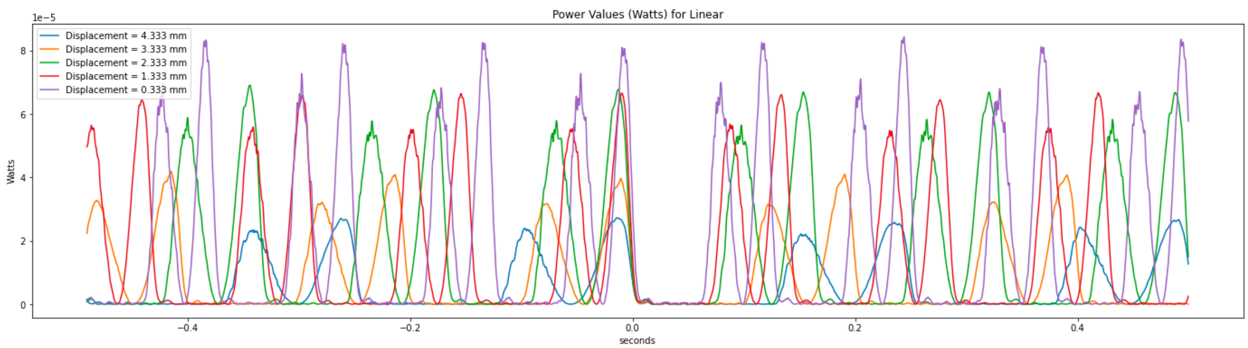

c. Effects of varying frequency on voltage output for linear.

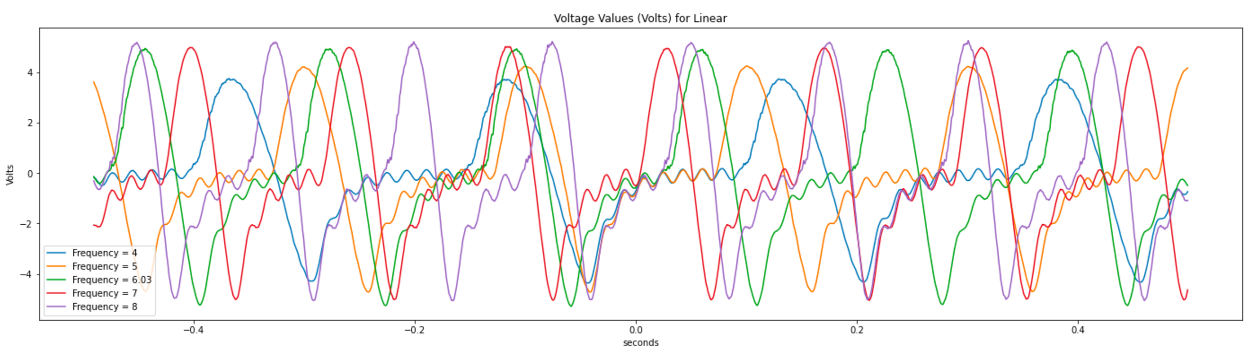

d. Effects of varying frequency on power output for linear.

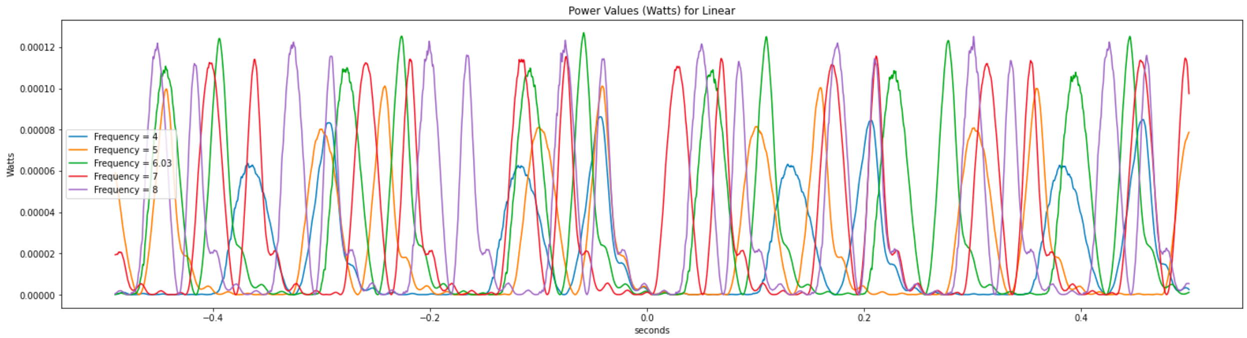
Power Values (Watts) for Linear
Watts
seconds
Frequency = 4
Frequency = 5
Frequency = 6.03
Frequency = 7
Frequency = 8
0.00012
0.00010
0.00008
0.00006
0.00004
0.00002
0.00000
−0.4
−0.2
0.0
0.2
0.4

Works Cited

[1] "Review of Power Quality Issues in Solar and Wind Energy," *Mater. Today Proc.*, vol. 24, pp. 2137–2143, Jan. 2020, doi: 10.1016/j.matpr.2020.03.670.

[2] A. (ORCID:000000025371917X) Dai, D. Luo, M. Song, and J. Liu, "Arctic amplification is caused by sea-ice loss under increasing CO2," *Nat. Commun.*, vol. 10, no. 1, Jan. 2019, doi: 10.1038/s41467-018-07954-9.

[3] S. Bukhary, S. Ahmad, and J. Batista, "Analyzing land and water requirements for solar deployment in the Southwestern United States," *Renew. Sustain. Energy Rev.*, vol. 82, pp. 3288–3305, Feb. 2018, doi: 10.1016/j.rser.2017.10.016.

[4] Y. (ORCID:0000000326670697) Zou, Y. (ORCID:0000000272902551) Wang, Z. (ORCID:0000000159825056) Xie, H. Wang, and P. J. Rasch, "Atmospheric teleconnection processes linking winter air stagnation and haze extremes in China with regional Arctic sea ice decline," *Atmospheric Chem. Phys. Online*, vol. 20, no. 8, Art. no. PNNL-SA-149191, Apr. 2020, doi: 10.5194/acp-20-4999-2020.

[5] A. Badel, A. Benayad, E. Lefeuvre, L. Lebrun, C. Richard, and D. Guyomar, "Single crystals and nonlinear process for outstanding vibration-powered electrical generators," *IEEE Trans. Ultrason. Ferroelectr. Freq. Control*, vol. 53, no. 4, pp. 673–684, Apr. 2006, doi: 10.1109/TUFFC.2006.1621494.

[6] A. Toprak and O. Tigli, "Piezoelectric energy harvesting: State-of-the-art and challenges," *Appl. Phys. Rev.*, vol. 1, no. 3, p. 031104, Sep. 2014, doi: 10.1063/1.4896166.

[7] Y. Oh *et al.*, "Flexible Energy Harvester with Piezoelectric and Thermoelectric Hybrid Mechanisms for Sustainable Harvesting," *Int. J. Precis. Eng. Manuf.-Green Technol.*, vol. 6, no. 4, pp. 691–698, Aug. 2019, doi: 10.1007/s40684-019-00132-2.

[8] J. Tichý*, J. Erhart, E. Kittinger*, and J. Přívratská, "Introduction to Phenomenological Crystal Structure," in *Fundamentals of Piezoelectric Sensorics: Mechanical, Dielectric, and Thermodynamical Properties of Piezoelectric Materials*, J. Tichý, J. Erhart, E. Kittinger, and J. Přívratská, Eds., Berlin, Heidelberg: Springer, 2010, pp. 15–29. doi: 10.1007/978-3-540-68427-5_2.

[9] P. Dhingra, "Energy Harvesting using Piezoelectric Materials," p. 5.

[10] R. M. Martin, "Piezoelectricity," *Phys. Rev. B*, vol. 5, no. 4, pp. 1607–1613, Feb. 1972, doi: 10.1103/PhysRevB.5.1607.

[11] H. Li, C. Tian, and Z. D. Deng, "Energy harvesting from low frequency applications using piezoelectric materials," *Appl. Phys. Rev.*, vol. 1, no. 4, p. 041301, Nov. 2014, doi: 10.1063/1.4900845.

[12] D. Damjanovic, "Contributions to the Piezoelectric Effect in Ferroelectric Single Crystals and Ceramics," *J. Am. Ceram. Soc.*, vol. 88, no. 10, pp. 2663–2676, 2005, doi: 10.1111/j.1551-2916.2005.00671.x.

[13] J. Wu, "Perovskite lead-free piezoelectric ceramics," *J. Appl. Phys.*, vol. 127, no. 19, pp. 1–13, May 2020, doi: 10.1063/5.0006261.

[14] A. Eddiai, M. Meddad, R. Farhan, M. Mazroui, M. Rguiti, and D. Guyomar, "Using PVDF piezoelectric polymers to maximize power harvested by mechanical structure," *Superlattices Microstruct.*, vol. 127, pp. 20–26, Mar. 2019, doi: 10.1016/j.spmi.2018.03.044.

[15] J. Tichý*, J. Erhart, E. Kittinger*, and J. Přívratská, "Elastic Properties of Crystals," in

Fundamentals of Piezoelectric Sensorics: Mechanical, Dielectric, and Thermodynamical Properties of Piezoelectric Materials, J. Tichý, J. Erhart, E. Kittinger, and J. Přívratská, Eds., Berlin, Heidelberg: Springer, 2010, pp. 31–53. doi: 10.1007/978-3-540-68427-5_3.

[16] R. Tavares and M. Ruderman, "Energy harvesting using piezoelectric transducers for suspension systems," *Mechatronics*, vol. 65, p. 102294, Feb. 2020, doi: 10.1016/j.mechatronics.2019.102294.

[17] "Piezoelectric Charge Constants." https://www.americanpiezo.com/knowledge-center/piezo-theory/piezoelectric-constants.html (accessed Oct. 24, 2020).

[18] H. Sodano, D. Inman, and G. Park, "A Review of Power Harvesting from Vibration using Piezoelectric Materials."

[19] M. D. Maeder, D. Damjanovic, and N. Setter, "Lead Free Piezoelectric Materials," *Kluwer Acad. Publ.*, vol. 13, no. Journal of Electroceramics, pp. 385–392, 2004.

[20] I. M. Reaney *et al.*, "Life cycle assessment and environmental profile evaluation of lead free piezeletrics in comparison with lead zirconate titanate," *J. Eur. Ceram. Soc.*, vol. 38, 2018.

[21] S. Zhang, R. Xia, L. Lebrun, D. Anderson, and T. Shrout, "Piezoelectric materials for high power, high temperature applications," *Elsevier*, Jun. 2005, doi: 10.1016/j.matlet.2005.06.016.

[22] M. Goldfarb and L. D. Jones, "On the Efficiency of Electric Power Generation With Piezoelectric Ceramic," *J. Dyn. Syst. Meas. Control*, vol. 121, no. 3, pp. 566–571, Sep. 1999, doi: 10.1115/1.2802517.

[23] S. Thomas R. and Z. Shujun J., "Lead-free piezoelectric ceramics: Alternatives for PZT?," *Springer*, 2007.

[24] R. Mahdi, N. J. Al-Bahnam, M. A. Ajeel, A. Al-Keisy, T. A. Hussein, and W. H. A. Majid, "High-performance (K,Na)NbO3-based binary lead-free piezoelectric ceramics modified with acceptor metal oxide," *Ceram. Int.*, vol. 46, no. 13, pp. 21762–21770, Sep. 2020, doi: 10.1016/j.ceramint.2020.05.287.

[25] S. Thomas R. and Z. Shujun J., "Lead-free piezoelectric ceramics: Alternatives for PZT?," *Springer*, 2007.

[26] P. K. Panda, "Review: environmentally friendly lead-free piezoelectric materials," *Springer*, Jul. 2009, doi: 10.1007/210853-009-3643-0.

[27] Z. Xu, W. Wang, J. Xie, Z. Xu, M. Zhou, and H. Yang, "An Impact-Based Frequency Up-Converting Hybrid Vibration Energy Harvester for Low Frequency Application.".

[28] X. Chen, T. Yang, W. Wang, and X. Yao, "Vibration energy harvesting with a clamped piezoelectric circular diaphragm," *Ceram. Int.*, vol. 38.

[29] J. Baker, S. Roundy, and P. Wright, "Alternative Geometries for Increasing Power Density in Vibration Energy Scavenging for Wireless Sensor Networks," in *3rd International Energy Conversion Engineering Conference*, San Francisco, California: American Institute of Aeronautics and Astronautics, Aug. 2005. doi: 10.2514/6.2005-5617.

[30] C. Covaci, I. Porobic, and A. Gontean, "Setup for Piezoelectric Energy Harvesting System," in *2019 IEEE 25th International Symposium for Design and Technology in Electronic Packaging (SIITME)*, Oct. 2019, pp. 78–81. doi: 10.1109/SIITME47687.2019.8990858.

[31] S. Chang, S. Ham, S. Kim, D. Suh, and H. Kim, "Ubi-Floor: Design and Pilot Implementation of an Interactive Floor System," in *2010 Second International Conference on Intelligent Human-Machine Systems and Cybernetics*, Aug. 2010, pp. 290–293. doi:

10.1109/IHMSC.2010.172.
[32] J. D. Mullen, "Maximizing power generation in and distributing force amongst piezoelectric generators," US7304416B2, Dec. 04, 2007 Accessed: Oct. 25, 2020. [Online]. Available: https://patents.google.com/patent/US7304416B2/en
[33] B. Kaur, A. Agnihotri, D. Thapar, and N. Arora, "Piezoelectric Energy Harvester Design and Power Conditioning with Solar Integration," in *2019 3rd International Conference on Electronics, Materials Engineering Nano-Technology (IEMENTech)*, Aug. 2019, pp. 1–6. doi: 10.1109/IEMENTech48150.2019.8981015.
[34] B. Yan, C. Zhang, L. Li, H. Zhang, and S. Deng, "Design and construction of magnetostrictive energy harvester for power generating floor systems," in *2015 18th International Conference on Electrical Machines and Systems (ICEMS)*, Oct. 2015, pp. 409–412. doi: 10.1109/ICEMS.2015.7385068.
[35] H. Zhao, Y. Tao, Y. Niu, and J. Ling, "Harvesting energy from asphalt pavement by piezoelectric generator," *J. Wuhan Univ. Technol.-Mater Sci Ed*, vol. 29, no. 5, pp. 933–937, Oct. 2014, doi: 10.1007/s11595-014-1023-3.
[36] M. J. Hessert, M. Vyas, J. Leach, K. Hu, L. A. Lipsitz, and V. Novak, "Foot pressure distribution during walking in young and old adults," *BMC Geriatr.*, vol. 5, p. 8, May 2005, doi: 10.1186/1471-2318-5-8.
[37] P. G. Weyand, B. R. Smith, M. R. Puyau, and N. F. Butte, "The mass-specific energy cost of human walking is set by stature," *J. Exp. Biol.*, vol. 213, no. 23, pp. 3972–3979, Dec. 2010, doi: 10.1242/jeb.048199.
[38] "Tech: Pavegen – the technology behind the tile | EG News," *EGi*, Apr. 10, 2017. https://www.egi.co.uk/news/pavegens-the-technology-behind-the-tile/ (accessed Mar. 28, 2023).
[39] A. M. Elhalwagy, M. Y. M. Ghoneem, and M. Elhadidi, "Feasibility Study for Using Piezoelectric Energy Harvesting Floor in Buildings' Interior Spaces," *Energy Procedia*, vol. 115, pp. 114–126, Jun. 2017, doi: 10.1016/j.egypro.2017.05.012.
[40] "Pavegen - Global leader in harvesting energy and data from footfall.," *Pavegen*. https://pavegen.com/ (accessed Oct. 14, 2020).
[41] E. L. Pradeesh and S. Udhayakumar, "Investigation on the geometry of beams for piezoelectric energy harvester," *Microsyst. Technol.*, vol. 25, no. 9, pp. 3463–3475, Sep. 2019, doi: 10.1007/s00542-018-4220-8.
[42] X. Luo, J. Wang, M. Dooner, and J. Clarke, "Overview of current development in electrical energy storage technologies and the application potential in power system operation," *Appl. Energy*, vol. 137, pp. 511–536, Jan. 2015, doi: 10.1016/j.apenergy.2014.09.081.
[43] B. Dunn, H. Kamath, and J.-M. Tarascon, "Electrical Energy Storage for the Grid: A Battery of Choices," *Science*, vol. 334, no. 6058, pp. 928–935, Nov. 2011, doi: 10.1126/science.1212741.
[44] A. Poullikkas, "A comparative overview of large-scale battery systems for electricity storage," *Renew. Sustain. Energy Rev.*, vol. 27, pp. 778–788, Nov. 2013, doi: 10.1016/j.rser.2013.07.017.
[45] B. Zakeri and S. Syri, "Electrical energy storage systems: A comparative life cycle cost analysis," *Renew. Sustain. Energy Rev.*, vol. 42, pp. 569–596, Feb. 2015, doi: 10.1016/j.rser.2014.10.011.
[46] C. S. Lai and M. D. McCulloch, "Levelized cost of electricity for solar photovoltaic and electrical energy storage," *Appl. Energy*, vol. 190, pp. 191–203, Mar. 2017, doi:

10.1016/j.apenergy.2016.12.153.
[47] H. L. Ferreira, R. Garde, G. Fulli, W. Kling, and J. P. Lopes, “Characterisation of electrical energy storage technologies,” *Energy*, vol. 53, pp. 288–298, May 2013, doi: 10.1016/j.energy.2013.02.037.
[48] “Sustainable Recycling Technology for Li-Ion Batteries and Beyond: Challenges and Future Prospects | Chemical Reviews.” https://pubs.acs.org/doi/10.1021/acs.chemrev.9b00535 (accessed Oct. 26, 2020).
[49] “Effective Recycling of Electric-vehicle Batteries | SpringerLink.” https://link.springer.com/article/10.1007/s38311-018-0139-z (accessed Oct. 26, 2020).
[50] J. Ajitsaria, “Modeling and analysis of a bimorph piezoelectric cantilever beam for voltage generation,” *IOPScience*, Accessed: Mar. 21, 2023. [Online]. Available: https://www.eng.auburn.edu/~choeson/Publication/1145_2007_Modeling%20and%20analysis%20of%20a%20bimorph%20piezoelectric%20_J.%20Ajitsaria.pdf